

Nonperturbative study of the two-frequency sine-Gordon model

Z. Bajnok^{1*}, L. Palla^{1†}, G. Takács^{2‡} and F. Wágner^{1§}

¹ Institute for Theoretical Physics, Eötvös University
H-1117 Budapest, Pázmány Péter sétány 1/A
Hungary

² Department of Mathematics, King’s College London
Strand, London WC2R 2LS, UK

October 31, 2018

Abstract

The two-frequency sine-Gordon model is examined. The focus is mainly on the case when the ratio of the frequencies is $1/2$, given the recent interest in the literature. We discuss the model both in a perturbative (form factor perturbation theory) and a nonperturbative (truncated conformal space approach) framework, and give particular attention to a phase transition conjectured earlier by Delfino and Mussardo. We give substantial evidence that the transition is of second order and that it is in the Ising universality class. Furthermore, we check the UV-IR operator correspondence and conjecture the phase diagram of the theory.

PACS codes: 64.60.Fr, 11.10.Kk

Keywords: nonintegrable field theory, two-frequency/double sine–Gordon model, form factors, truncated conformal space approach, finite size effects, phase transition

*bajnok@poe.elte.hu

†palla@ludens.elte.hu

‡takacs@mth.kcl.ac.uk

§wferi@afavant.elte.hu

1 Introduction

The sine-Gordon model has attracted a great deal of interest over the decades, for the particular reason that while being an integrable field theory, it can be used as a toy model for many nonperturbative quantum field theory phenomena. It also has very interesting applications in diverse areas of physics, ranging from statistical mechanics of one-dimensional quantum spin chains to nonlinear optics (for a – non-exhaustive, but representative – list with references see the introduction of [1]).

In the present paper we study a nonintegrable extension of sine-Gordon theory in which the scalar potential consists of two cosine terms with different frequencies, called the two-frequency or double sine-Gordon (DSG) model. It is suggested in [1] that this model can be used as a more refined approximation to some of the physical situations (e.g. wave propagation in a nonlinear medium) where the ordinary sine-Gordon model is applicable. The model is also interesting theoretically, since due to its nonintegrability it is expected to have more general behaviour than usual sine-Gordon theory and therefore it can be seen as a more realistic toy model for nonperturbative quantum field theory. Applications to the study of massive Schwinger model (two-dimensional quantum electrodynamics) and a generalized Ashkin-Teller model (a quantum spin system) are discussed in [1] and another potentially interesting application to the one-dimensional Hubbard model is examined in [2] (together with the generalized Ashkin-Teller model mentioned above). A further potentially interesting application of the two-(and multi-)frequency sine-Gordon model is for ultra-short optical pulses propagating in resonant degenerate medium [3].

We show that for a rational ratio of the frequencies this model is still amenable to a nonperturbative treatment using the truncated conformal space approach (TCSA), and that a great deal of interesting information can be extracted, in particular the existence and the characteristics of a phase transition which was predicted in [1] on the basis of simple classical (mean field) arguments.

The outline of the paper is as follows. In Section 2 we introduce the model and discuss some of its basic features. Then in Section 3 we set up the TCSA framework for the model. Section 4 discusses results obtained from the so-called form factor perturbation theory (FFPT), while in Section 5 we compare the FFPT results to the numerical data resulting from TCSA in order to test the reliability of the latter method. Section 6 is devoted to a preliminary discussion of phase transition in the case when the ratio of the two frequencies is $1/2$ (denoted by DSG_2) and contains a general analysis of signatures of second and first order phase transitions in finite volume in a separate subsection. In Section 7 we apply these general considerations to construct the phase diagram of the model DSG_2 and then we make our conclusions in Section 8. The paper contains an Appendix which collects the formulas used for computing the first order corrections in form factor perturbation theory.

2 The two-frequency sine-Gordon model

2.1 Definition of the model

The two-frequency sine-Gordon (or double sine-Gordon, DSG) model is defined by the action

$$\mathcal{A}_{\text{DSG}} = \int dt \int dx \left(\frac{1}{2} \partial_\mu \Phi \partial^\mu \Phi + \mu \cos \beta \Phi + \lambda \cos (\alpha \Phi + \delta) \right), \quad (2.1)$$

where β, α are the two frequencies, μ, λ are dimensionful couplings (classically of dimension mass²) and δ is a relative phase. Setting μ or λ to zero the DSG model reduces to an ordinary sine-Gordon model.

At the quantum level this theory can be considered as a double perturbation of its $c = 1$ UV limiting conformal field theory. The action can be written in the following form

$$\mathcal{A}_{\text{DSG}} = \mathcal{A}_{c=1} - \mathcal{A}_{\text{pert}}, \quad (2.2)$$

where

$$\mathcal{A}_{c=1} = \int dt \int dx \frac{1}{2} \partial_\mu \Phi \partial^\mu \Phi, \quad (2.3)$$

$$\mathcal{A}_{\text{pert}} = -\frac{1}{2} \int dt \int dx (\mu V_\beta + \mu V_{-\beta} + \lambda e^{i\delta} V_\alpha + \lambda e^{-i\delta} V_{-\alpha}), \quad (2.4)$$

and V_ω denotes the exponential field (vertex operator)

$$V_\omega = e^{i\omega \Phi}, \quad (2.5)$$

which in the UV limit corresponds to a ($\widehat{U(1)}$ Kac-Moody) primary field with conformal dimensions

$$\Delta_\omega^\pm = \Delta_\omega = \frac{\omega^2}{8\pi}, \quad (2.6)$$

where the upper index \pm corresponds to the right/left conformal algebra. Correspondingly the couplings at the quantum level have the following dimensions

$$[\mu] = (\text{mass})^{2-2\Delta_\beta}, \quad (2.7)$$

$$[\lambda] = (\text{mass})^{2-2\Delta_\alpha}. \quad (2.8)$$

We also introduce two mass scales M_α and M_β , which are defined to be the masses of the sine-Gordon solitons in the models with $\mu = 0$ or $\lambda = 0$, respectively. It is known [4] that these masses are related to the couplings λ, μ via

$$\begin{aligned} \mu &= \kappa_\beta M_\beta^{2-2\Delta_\beta}, \\ \lambda &= \kappa_\alpha M_\alpha^{2-2\Delta_\alpha}, \end{aligned} \quad (2.9)$$

where

$$\kappa_\omega = \frac{2\Gamma(\Delta_\omega)}{\pi\Gamma(1-\Delta_\omega)} \left(\frac{\sqrt{\pi}\Gamma\left(\frac{1}{2-2\Delta_\omega}\right)}{2\Gamma\left(\frac{\Delta_\omega}{2-2\Delta_\omega}\right)} \right)^{2-2\Delta_\omega}. \quad (2.10)$$

2.2 General properties of the model

The DSG model was examined in [1] by Delfino and Mussardo, where some general observations were made. Here we recall these facts without eventually going into any details.

The first observation is a simple consequence of the formulation of the model as a perturbed $c = 1$ CFT. Namely, in order for the two perturbing operators to be relevant, one has to restrict

$$\beta^2 \leq 8\pi \quad , \quad \alpha^2 \leq 8\pi . \quad (2.11)$$

Furthermore, we assume that the theory is renormalizable in the strict sense, i.e. all divergences can be absorbed into redefining the coupling constants μ and λ (otherwise one needs to add new (periodic) counterterms to the action and the theory is no more a two-frequency sine-Gordon model but rather some multi-frequency version). This means that we have to restrict

$$\alpha\beta \leq 4\pi . \quad (2.12)$$

In the sequel we always assume that the above two conditions hold.

Another nontrivial property of the model is that it is a nonintegrable field theory¹ if $\alpha \neq \beta$ and both couplings λ , μ are nonzero. In addition, the model exhibits drastically different behaviour depending on whether the ratio of the two frequencies is rational or irrational.

2.2.1 Rational case

If

$$\frac{\alpha}{\beta} = \frac{m}{n} \quad (2.13)$$

with m and n two relative prime positive integers, then the potential $-\mu \cos \beta\Phi - \lambda \cos (\alpha\Phi + \delta)$ is periodic with period

$$\frac{2\pi n}{\beta} = \frac{2\pi m}{\alpha} . \quad (2.14)$$

It can then be shown that the fundamental range of the δ parameter is

$$|\delta| \leq \frac{\pi}{n} \quad (2.15)$$

(i.e. any model with other values of the parameter δ can be redefined into one with a δ lying in the fundamental range by shifting the field with some integer multiple of $\frac{2\pi}{\beta}$). The periodicity of the potential implies that the theory has an infinitely degenerate ground state and supports topologically charged excitations. The fundamental topological excitation degenerates in the $\lambda = 0$ limit to an n -soliton state of the corresponding sine-Gordon theory and similarly for the $\mu = 0$ limit it is an m -soliton state. For general values of the couplings, the solitons are in a sense “confined” into these composite objects.

¹One can argue for the nonintegrability e.g. noting that the so-called “counting argument” fails to provide any conserved higher spin quantities if $\alpha \neq \beta$ and both λ and μ are nonzero.

2.2.2 Irrational case

If, on the other hand,

$$\frac{\alpha}{\beta} \notin \mathbb{Q}, \quad (2.16)$$

then the potential is not periodic. There are no topologically charged excitations and the solitons are completely confined. Delfino and Mussardo [1] argue that in this case the ground state is unique. Furthermore, from (2.15) we can infer that the parameter δ presumably plays no role in the dynamics of the model.

The irrational case is extremely complicated, even as a quantum mechanical problem (i.e. neglecting the x dependence). In the next section we shall see that it is impossible to apply the well-known TCOSA method in this case and in lack of any alternative nonperturbative method in the present paper we restrict our attention to the rational case (although the perturbative formulas presented in Section 4 apply in the irrational case as well).

3 Truncated Conformal Space Approach

Here we only review the specifics of TCOSA as applied to the DSG model. This nonperturbative (numerical) method was invented by Yurov and Zamolodchikov in [5] and extended to $c = 1$ theories in [6] to which we refer the interested reader for more details.

3.1 The UV Hilbert space

The first important issue is the operator content of the UV limiting $c = 1$ CFT. We need a theory in which the perturbing operators $V_{\pm\alpha}$, $V_{\pm\beta}$ correspond to local operators.

In the $c = 1$ CFT we consider the spectrum of local operators is generated by the conformal families of $\widehat{U(1)}$ Kac-Moody primary fields $\mathcal{V}_{r,s}$ with scaling dimensions

$$\Delta_{r,s}^{\pm} = \frac{1}{2} \left(\frac{r}{R} \pm \frac{1}{2} s R \right)^2, \quad r, s \in \mathbb{Z}, \quad (3.1)$$

where R is the compactification radius of the $c = 1$ free boson field χ with the action

$$\mathcal{A}_{\chi} = \frac{1}{8\pi} \int d^2x \partial_{\mu} \chi \partial^{\mu} \chi, \quad \chi \sim \chi + 2\pi R. \quad (3.2)$$

Taking into account eqn. (2.13) and the fact that the normalization of Φ and χ differ by $\sqrt{4\pi}$, their identification is essentially unique up to a positive integer k :

$$R = k \frac{\sqrt{4\pi n}}{\beta} = k \frac{\sqrt{4\pi m}}{\alpha}, \quad (3.3)$$

$$V_{\pm\beta} \equiv \mathcal{V}_{\pm nk, 0}, \quad V_{\pm\alpha} \equiv \mathcal{V}_{\pm mk, 0}. \quad (3.4)$$

The integer k is the folding number, which has been considered in the context of sine-Gordon theory in [7] and can be introduced in any scalar field theory with periodic potential: it corresponds to identifying the field as an angular variable after k periods of the potential. We choose $k = 1$, which means we identify

$$\Phi \equiv \Phi + \frac{2\pi n}{\beta} l \quad , \quad l \in \mathbb{Z} . \quad (3.5)$$

However, it can now be seen that in the limit $\lambda = 0$ we recover an n -folded version of sine-Gordon theory (denoted $\text{SG}(\beta, n)$ in [7]) while in the $\mu = 0$ case we get the theory $\text{SG}(\alpha, m)$. We remark that by choosing $k = 1$ we do not lose any information on the DSG model, since the other $k > 1$ folded versions can be obtained from the $k = 1$ case by adding some twisted sectors as in [7]. However, we shall see that the fact that the sine-Gordon limits are in general *folded models* will play a very important role in the dynamics of the DSG model. There is also a fermionic version of the theory which has primary fields $\mathcal{V}_{r,s}$ in the UV with

$$s \in \mathbb{Z} \quad , \quad r \in \mathbb{Z} + \frac{s}{2} \quad (3.6)$$

but similarly to the folded ones, this version can be constructed by replacing some of the topologically charged sectors with some (fermionic) twisted ones. As we are only interested in the dynamics of the vacuum sector we shall not discuss this modification here either.

We also wish to note that as the irrational case can be considered as a limit $n, m \rightarrow \infty$, the Hilbert space of the irrational DSG model corresponds to an uncompactified boson in the ultraviolet limit, with a continuous spectrum of primary fields

$$\mathcal{V}_{r,0} \quad , \quad \Delta_r^\pm = \frac{r^2}{2} \quad , \quad r \in \mathbb{R} . \quad (3.7)$$

The fact that the spectrum is continuous means that TCSA is not applicable since the conformal Hilbert space contains infinitely many states even when truncated by imposing some upper bound on conformal energy.

3.2 The TCSA Hamiltonian

We put the system on a cylinder with finite spatial volume L , i.e. we take the space coordinate $0 \leq x < L$ and identify x with $x + L$. Given the identification (3.5) this means in fact the following quasi-periodic boundary condition for the field Φ :

$$\Phi(x + L) = \Phi(x) + \frac{2\pi n}{\beta} q \quad , \quad q \in \mathbb{Z} . \quad (3.8)$$

q is the winding number labelling different sectors of the theory, and corresponds to a conserved topological charge in the full perturbed CFT. In the present paper we are only interested in the $q = 0$ sector as it contains all the relevant information for the problems

treated in this work. In addition, in the sector containing the vacuum the Lorentz spin of all the states is also zero, i.e. $(L_0 - \bar{L}_0) |\Psi\rangle = 0$ for any state $|\Psi\rangle$.

After a mapping onto the conformal plane, the Hamiltonian of the theory can be written in the following form

$$H_{\text{DSG}} = \frac{2\pi}{L} \left(L_0 + \bar{L}_0 - \frac{c}{12} + \frac{\mu L^{2-2\Delta_\beta}}{2(2\pi)^{1-2\Delta_\beta}} (V_\beta(1) + V_{-\beta}(1)) + \frac{\lambda L^{2-2\Delta_\alpha}}{2(2\pi)^{1-2\Delta_\alpha}} (V_\alpha(1) + V_{-\alpha}(1)) \right) \quad (3.9)$$

The matrix elements of this operator can be calculated explicitly between any two states in the UV limiting Hilbert space. Truncating this space to finitely many state by introducing an upper conformal energy cutoff the Hamiltonian becomes a finite matrix, which can then be diagonalized numerically to get an approximation of the spectrum. Thus one can extract the energy $E_\Psi(L)$ of any state Ψ as a function of the volume L .

It is well-known [8] that TCSA suffers from UV divergences whenever the scaling dimension $\Delta^+ + \Delta^-$ of any of the perturbing operators is larger than 1. In this case the only quantities that are possible to extract are the energies relative to the ground state i.e. $E_i(L) - E_0(L)$. Furthermore, in the case where TCSA is UV divergent the truncation errors are much larger even for such relative energies, and grow very fast with the volume L , which restricts the usefulness of TCSA in this case to small values of L .

3.3 The interpolating mass scale

In order to get numerical results, we have to fix the units in which we measure energies and distances. For later convenience, we introduce the following ‘*interpolating*’ mass scale

$$M = \frac{M_\beta \mu^{x_\alpha} + M_\alpha \lambda^{x_\beta}}{\mu^{x_\alpha} + \lambda^{x_\beta}}, \quad (3.10)$$

where $x_\omega = 2 - 2\Delta_\omega$. We also use the following dimensionless combination of the coupling constants

$$\eta = \frac{\lambda^{x_\beta}}{\mu^{x_\alpha} + \lambda^{x_\beta}}. \quad (3.11)$$

The advantage of this parametrization is that M interpolates smoothly between the mass scales of the two limiting sine-Gordon models, which correspond to $\eta = 0$ and 1, respectively. Introducing the notation

$$D = \frac{(1 - \eta)^{1 + \frac{1}{x_\alpha x_\beta}}}{\kappa_\beta^{\frac{1}{x_\beta}}} + \frac{\eta^{1 + \frac{1}{x_\alpha x_\beta}}}{\kappa_\alpha^{\frac{1}{x_\alpha}}}, \quad (3.12)$$

we obtain

$$\mu = \frac{M^{x_\beta} (1 - \eta)^{\frac{1}{x_\alpha}}}{D^{x_\beta}}, \quad \lambda = \frac{M^{x_\alpha} \eta^{\frac{1}{x_\beta}}}{D^{x_\alpha}}, \quad (3.13)$$

and the Hamiltonian can be made dimensionless as follows:

$$h_{\text{DSG}} = \frac{1}{M} H_{\text{DSG}} = \frac{2\pi}{l} \left(L_0 + \bar{L}_0 - \frac{c}{12} + \frac{(1-\eta)^{\frac{1}{x_\alpha}}}{2(2\pi)^{x_\beta-1}} \left(\frac{l}{D} \right)^{x_\beta} (V_\beta(1) + V_{-\beta}(1)) + \frac{\eta^{\frac{1}{x_\beta}}}{2(2\pi)^{x_\alpha-1}} \left(\frac{l}{D} \right)^{x_\alpha} (V_\alpha(1) + V_{-\alpha}(1)) \right), \quad (3.14)$$

where we introduced the dimensionless volume parameter

$$l = ML. \quad (3.15)$$

We denote the eigenvalue of h_{DSG} corresponding to the state Ψ and as a function of l by $\epsilon_\Psi(l)$ i.e. $E_\Psi(L) = M\epsilon_\Psi(ML)$.

It is very important that h_{DSG} interpolates smoothly between the two extremal sine-Gordon models as η varies from 0 to 1. Had we chosen as our units one of the soliton mass scales M_β or M_α , the dimensionless Hamiltonian would have been singular at the other end of the η interval. We shall discuss that there is a little inconvenience in the choice (3.10) when we want to compare with perturbation theory around one of the end points, since such a calculation is more naturally formulated in terms of the mass scale of the corresponding extremal sine-Gordon model rather than the interpolating mass scale. However, the convenience of being able to scan the whole range of η with a single numerical program well outweighs this disadvantage.

4 Form factor perturbation theory

4.1 Generalities

To supplement and check TCSA (which is a numerical method) with some analytic results, we use the so-called *form factor perturbation theory* (FFPT). The viewpoint of considering a nonintegrable field theory as a perturbation of an integrable one was first taken in [9] to which we refer the reader for a detailed exposition of the subject. Here we restrict ourselves to a brief summary of the necessary formulae.

Consider an integrable quantum field theory with action \mathcal{A}_0 perturbed by a spinless local field $\Psi(x)$:

$$\mathcal{A} = \mathcal{A}_0 - g \int d^2x \Psi(x). \quad (4.1)$$

Assume that the spectrum of the unperturbed theory \mathcal{A}_0 is known, together with the following matrix elements of $\Psi(x)$ (form factors):

$$F_{a_1 \dots a_n}^\Psi(\vartheta_1, \dots, \vartheta_n)_0 = {}_0\langle 0 | \Psi(0) | a_1(\vartheta_1) \dots a_n(\vartheta_n) \rangle_0^{\text{in}}, \quad (4.2)$$

where $|0\rangle_0$ is the vacuum state and $|a_1(\vartheta_1)\dots a_n(\vartheta_n)\rangle_0^{\text{in}}$ denotes an asymptotic n -particle in-state of particles a_1, \dots, a_n with rapidities β_1, \dots, β_n in the unperturbed theory \mathcal{A}_0 . Using FFPT one can calculate the spectrum of the theory \mathcal{A} perturbatively in the coupling constant g . Here we list the results obtained to first order. The vacuum energy density is shifted by an amount

$$\delta\mathcal{E}_{\text{vac}} = g {}_0\langle 0|\Psi|0\rangle_0. \quad (4.3)$$

The mass (squared) matrix M_{ab}^2 gets a correction

$$\delta M_{ab}^2 = 2g F_{ab}^\Psi(i\pi, 0) \delta_{m_a, m_b} \quad (4.4)$$

supposing that the original mass matrix was diagonal and of the form

$$M_{ab}^2 = m_a^2 \delta_{ab}. \quad (4.5)$$

Finally, the scattering amplitude for the four particle process $a + b \rightarrow c + d$ is modified by

$$\delta S_{ab}^{cd}(\vartheta) = -ig \frac{F_{cdab}^\Psi(i\pi, \vartheta + i\pi, 0, \vartheta)}{m_a m_b \sinh \vartheta}, \quad \vartheta = \vartheta_a - \vartheta_b. \quad (4.6)$$

4.2 Analytic results

Using the general formulas above and the ones for the form factors and vacuum expectation values, listed in Appendix A, one can derive analytic formulas for the first order corrections to the vacuum energy density and the spectrum.

We identify the unperturbed theory and the perturbing operator in the following way:

$$\mathcal{A}_0 = \int dt \int dx \left(\frac{1}{2} \partial_\mu \Phi \partial^\mu \Phi + \mu : \cos \beta \Phi : \right) \quad (4.7)$$

$$\Psi(x) =: \cos(\alpha \Phi + \delta) : , \quad g = -\lambda. \quad (4.8)$$

We recall that

$$\frac{\alpha}{\beta} = \frac{m}{n}, \quad m, n \in \mathbb{N} \quad (4.9)$$

and we denote the soliton mass in the unperturbed theory \mathcal{A}_0 by M_β , as in Subsection 2.1. Now it is straightforward to apply the general formulae summarized above, however, some care must be taken since in the unperturbed theory ($\lambda = 0$) the vacuum and the breather states come in n -fold degenerate multiplets reflecting the folded nature of the limiting SG model. When the perturbation is switched on ($\lambda \neq 0$) it not only shifts the vacuum energy density and the masses but also removes (possibly part of) the degeneracies.

Note that it is possible to interchange the role of the two cosine terms and therefore there are eventually two perturbative regimes of the model. We present the formulas for

the above assignment; it is a trivial matter (by suitably shifting the field and redefining the δ phase parameter) to get the formulae corresponding to the other possibility. We also frequently use the parameter

$$p = \frac{\beta^2}{8\pi - \beta^2} . \quad (4.10)$$

4.2.1 Vacuum energy densities

First we discuss the shift in the vacuum energy density. From (3.5) we see that the model \mathcal{A}_0 has n vacua $|k\rangle$, $k = 0, \dots, n-1$, characterized by

$$\langle k | \Phi(x) | k \rangle = \frac{2\pi}{\beta} k . \quad (4.11)$$

In infinite volume, no local operator has nonzero matrix elements between $|k\rangle$ and $|k'\rangle$ for $k \neq k'$; therefore, the perturbative formulas can be applied for each state $|k\rangle$ straightforwardly. This applies to all excited states above the vacua $|k\rangle$ as well (see e.g. the breathers in the next subsection). According to (4.3) the vacuum energy density of the k th vacuum is shifted by

$$\delta\mathcal{E}_k = -\frac{\lambda}{2} \left(e^{i\delta} \mathcal{G}_\alpha^{(k)}(\beta) + e^{-i\delta} \mathcal{G}_{-\alpha}^{(k)}(\beta) \right) , \quad \mathcal{G}_\alpha^{(k)}(\beta) = \langle k | e^{i\alpha\Phi(0)} | k \rangle . \quad (4.12)$$

Using (A.4, A.25) we obtain the final form

$$\delta\mathcal{E}_k = -\lambda \mathcal{G}_\alpha(\beta) \cos \left(\frac{2\pi\alpha}{\beta} k + \delta \right) , \quad (4.13)$$

where $\mathcal{G}_\alpha(\beta) = \mathcal{G}_\alpha^{(0)}(\beta)$. We remark that one can extract a similar result from the classical potential

$$V(\Phi) = -\mu \cos \beta\Phi - \lambda \cos(\alpha\Phi + \delta) . \quad (4.14)$$

At $\lambda = 0$, the minima are

$$\Phi_k^{(0)} = \frac{2\pi k}{\beta} , \quad V(\Phi_k^{(0)}) = -\mu . \quad (4.15)$$

Switching on a small λ , the minima are shifted to

$$\Phi_k = \Phi_k^{(0)} + \delta\Phi_k , \quad \delta\Phi_k = -\lambda \frac{\alpha}{\mu\beta^2} \sin \left(2\pi k \frac{\alpha}{\beta} + \delta \right) + O(\lambda^2) \quad (4.16)$$

and the new values of the potential at these minima are

$$V(\Phi_k) = -\mu - \lambda \cos \left(\frac{2\pi\alpha}{\beta} k + \delta \right) . \quad (4.17)$$

Therefore we obtain

$$\delta\mathcal{E}_k^{\text{classical}} = -\lambda \cos\left(\frac{2\pi\alpha}{\beta}k + \delta\right), \quad (4.18)$$

which is exactly the classical limit of (4.13) since it can be easily proven from (A.4) that

$$\mathcal{G}_\alpha(\beta) \rightarrow 1 \quad \text{as} \quad \beta \rightarrow 0 \quad , \quad \frac{\alpha}{\beta} = \text{fixed}. \quad (4.19)$$

4.2.2 Mass corrections

We calculate the first order corrections to the masses of the first and the second breathers, M_1 and M_2 . In general

$$\delta M_r = \frac{\delta M_r^2}{2M_r} = \frac{\delta M_r^2}{4M_\beta \sin \frac{r p \pi}{2}}, \quad (4.20)$$

where, as before, M_β is the soliton mass in the unperturbed theory $\lambda = 0$.

Eventually, there are n copies of each breather: $B_r^{(k)}$ is the r th breather living over the vacuum $|k\rangle$, $k = 0, \dots, n-1$ (c.f. [7]). In the theory \mathcal{A}_0 , their masses are independent of k , but the degeneracy is split by the perturbing potential. We denote the corresponding mass corrections by $\delta M_r^{(k)}$. The masses of the first and second breathers can be calculated using (4.4) and (A.8, A.22) and turn out to be

$$\delta M_1^{(k)} = \frac{\lambda \mathcal{G}_\alpha(\beta) \mathcal{N}}{M_\beta} \cos\left(\frac{2\pi\alpha}{\beta}k + \delta\right) \frac{\sin^2\left(p\pi\frac{\alpha}{\beta}\right)}{\sin^2\left(\frac{p\pi}{2}\right)} \exp\left\{-\frac{1}{\pi} \int_0^{p\pi} dt \frac{t}{\sin t}\right\}, \quad (4.21)$$

$$\begin{aligned} \delta M_2^{(k)} &= \frac{\lambda \mathcal{G}_\alpha(\beta) \mathcal{N}^2}{M_\beta} \cos\left(\frac{2\pi\alpha}{\beta}k + \delta\right) \frac{\sin^2\left(p\pi\frac{\alpha}{\beta}\right)}{\sin^2\left(\frac{p\pi}{2}\right) \cos(p\pi)} \times \\ &\quad \left(2 \cos^2\left(\frac{p\pi}{2}\right) - \sin^2\left(p\pi\frac{\alpha}{\beta}\right)\right) \exp\left\{-\frac{2}{\pi} \int_0^{p\pi} dt \frac{t}{\sin t}\right\}, \end{aligned} \quad (4.22)$$

(the constant \mathcal{N} is defined in (A.14)).

One can also do a semiclassical analysis for the first breather mass. We remark that the first breather is identified with the particle created by the fundamental scalar field Φ and therefore its mass is given by the second derivative of the potential V at its minima. Explicitly we obtain

$$M_1^{(k)} = \sqrt{\mu}\beta + \lambda \frac{\alpha^2}{2\sqrt{\mu}\beta} \cos\left(\frac{2\pi\alpha}{\beta}k + \delta\right) + O(\lambda^2), \quad (4.23)$$

which can be matched with the classical limit $\beta \rightarrow 0$ of (4.21) using

$$M_\beta^{\text{classical}} = \frac{8\sqrt{\mu}}{\beta}, \quad (4.24)$$

and $\mathcal{N} \rightarrow 1$ as $\beta \rightarrow 0$ following from (A.14).

4.2.3 S-matrix corrections

We can also compute the first order correction to the $B_1 - B_1$ S-matrix, using (4.6, A.9). The result is

$$\delta S_{11}(\vartheta) = i \frac{\lambda \mathcal{G}_\alpha(\beta) \mathcal{N}^2}{M_\beta^2} \cos\left(\frac{2\pi\alpha}{\beta} k + \delta\right) S_{11}(\vartheta) \frac{4 \cos^2\left(\frac{p\pi}{2}\right) \sin^2\left(p\pi \frac{\alpha}{\beta}\right)}{\sin^2\left(\frac{p\pi}{2}\right)} \times \quad (4.25)$$

$$\left(\frac{\sin^2\left(p\pi \frac{\alpha}{\beta}\right)}{\sin^2(p\pi)} - \frac{1}{\cosh(\vartheta) + 1}\right) \frac{\sinh \vartheta}{\sinh^2 \vartheta + \sin^2(p\pi)} \quad (4.26)$$

where

$$S_{11}(\vartheta) = \frac{\sinh \vartheta + i \sin p\pi}{\sinh \vartheta - i \sin p\pi} \quad (4.27)$$

is the sine-Gordon $B_1 - B_1$ S-matrix. It turns out, however, that this correction is too small and cannot be measured within the precision of TCSEA.

5 Comparison of FFPT with TCSEA

5.1 Extracting the vacuum energy densities and the mass spectrum from TCSEA

TCSEA gives the spectrum of the dimensionless Hamiltonian h_{TCSEA} (3.14) as a function of the dimensionless volume parameter l (3.15). In our numerical calculations, we use the interpolating mass scale M (3.10) as a unit of mass. However, the FFPT results are expressed in terms of the scale M_β ; we must therefore take care of converting between the two conventions. We describe first how we extract the vacuum energy densities and the various masses from the TCSEA data then we compare these ‘experimentally measured’ quantities and the FFPT predictions on a specific example when $\alpha/\beta = 1/2$.

5.1.1 Vacuum energy density

Concerning the vacuum energy density, our numerical results show that the ground state energy is linear in the volume L

$$E_{\text{vac}} = \mathcal{E}_{\text{vac}} L \quad (5.1)$$

for a wide range of L . Therefore the (dimensionless) vacuum energy density $\mathcal{E}_{\text{vac}}/M^2$ can be measured as $\epsilon_{\text{vac}}(l_0)/l_0$ by choosing some value l_0 in this range (typically between 14 and 20). We extract the shift in the vacuum energy density using the relation

$$\frac{\delta \mathcal{E}_{\text{vac}}}{M_\beta^2} = \frac{\epsilon_{\text{vac}}(l_0)}{l_0} \left(\frac{M}{M_\beta}\right)^2 - \frac{\mathcal{E}_{\text{vac}}^{(0)}}{M_\beta^2} \quad (5.2)$$

where $\mathcal{E}_{\text{vac}}^{(0)}$ is the value measured using TCSA in the unperturbed theory at $\eta = 0$. It's value is known analytically as well

$$\frac{\mathcal{E}_{\text{vac}}^{(0)}}{M_\beta^2} = -\frac{1}{4} \tan \frac{p\pi}{2}, \quad (5.3)$$

however, we prefer to use the value extracted numerically because it helps eliminating part of the truncation error coming from TCSA.

5.1.2 Masses

We know that the energy of a particle a of momentum 0 in finite volume, relative to the ground state, has the form

$$E_a(L) - E_{\text{vac}}(L) = M_a + O(e^{-ML}) \quad (5.4)$$

where M_a is the mass of the particle and M is some mass scale characterizing the theory. As the interpolating scale (3.10) agrees with the relevant scales at the two extremal points $\eta = 0$ and $\eta = 1$, while in between it interpolates smoothly between them, we can take it as the characteristic scale of the DSG model. Therefore the simplest way to measure the mass is to extract it as the value of the energy above the ground state at a suitable value of the volume in a range (the scaling region) where the energy difference $E_a(L) - E_{\text{vac}}(L)$ is approximately constant; (however, this volume cannot be too large since then truncation errors would spoil the measurement). Therefore to obtain the mass corrections we use the relation

$$\frac{\delta M_a}{M_\beta} = (\epsilon_a(l_0) - \epsilon_{\text{vac}}(l_0)) \frac{M}{M_\beta} - \frac{M_a^{(0)}}{M_\beta} \quad (5.5)$$

where l_0 is a suitable value of the volume parameter, $\epsilon_a(l_0)$ is the relevant eigenvalue of (3.14) and $M_a^{(0)}$ is the mass measured at $\eta = 0$. Once again, the mass ratios

$$\frac{M_a^{(0)}}{M_\beta} \quad (5.6)$$

are known analytically, but we use the values extracted from TCSA in order to eliminate part of the numerical errors.

5.2 A special case: $\alpha = \beta/2$

We present the comparison between the numerical TCSA data and the analytical first order FFPT results for a special ratio of the frequencies. The reason for choosing this example is that (1) it is the simplest possible case and (2) this is the one that we treat nonperturbatively in detail later on. Let us first discuss the model itself. The action is

$$\mathcal{A} = \int dt \int dx \left(\frac{1}{2} \partial_\mu \Phi \partial^\mu \Phi + \mu \cos \beta \Phi + \lambda \cos \left(\frac{\beta}{2} \Phi + \delta \right) \right) \quad (5.7)$$

We denote this model by $\text{DSG}_2^\eta(\beta, \delta)$ (sometimes omitting the parameters in the parentheses). The field is defined as an angular variable (3.5), in this case with the period

$$\Phi \equiv \Phi + \frac{4\pi}{\beta}l \quad , \quad l \in \mathbb{Z} . \quad (5.8)$$

Therefore the theory $\text{DSG}_2^{\eta=0}$ has two vacua, which are degenerate in infinite volume and correspond to the classical minima

$$\Phi_0 = 0 \quad , \quad \Phi_1 = \frac{2\pi}{\beta} , \quad (5.9)$$

thus this model corresponds to a 2-folded sine-Gordon theory $\text{SG}(\beta, 2)$ [7]. The other extremal case $\text{DSG}_2^{\eta=1}$ has only one vacuum

$$\Phi'_0 = -\frac{2\delta}{\beta} \quad (5.10)$$

and is a 1-folded model $\text{SG}(\beta/2, 1)$.

In the vacuum sector of $\text{SG}(\beta, 2)$, every state essentially appears in two copies, corresponding to the two different vacua. In infinite volume, these copies are degenerate, but the degeneracy is lifted for finite L by the tunnelling between the two vacua. In particular, the vacua and the (neutral) one-particle states are split by an amount decreasing exponentially with the volume L . Switching on the perturbation removes this degeneracy in an interesting way.

Let us first discuss the case $\delta = 0$. Switching on λ , the two vacua have different vacuum energy densities and thus the leading term in the split between the two ground states becomes a term linear in L . To first order in λ , we obtain from (4.13)

$$E_{\text{vac}}^{(1)}(L) - E_{\text{vac}}^{(0)}(L) = 2\lambda\mathcal{G}_{\beta/2}(\beta)L + \dots \quad (5.11)$$

where $E^{(0,1)}(L)$ are the energies of the two vacuum states (Casimir energies) as functions of L and the ellipses denote terms which fall off exponentially with the volume. Since the vacuum energy density is universal for all excitations lying above the same ground state, the space of states separates into two parts which manifest themselves as lines with two different slopes in the large volume limit. In infinite volume, the Hilbert space of the system eventually reduces to the ones with the smaller slope, as the other set of states will lie at infinitely high energy above them. For this reason we call the states with the larger value of the vacuum energy density “*runaway*” states.

Of course, higher order terms modify the linear dependence of the slope on λ . In the other extremal point $\text{DSG}_2^{\eta=1}$ one has only one vacuum, but, as the corresponding sine-Gordon model is more attractive, it has more breather states. This is where the interpolating mass parameter (3.10) comes in handy: as the Hamiltonian (3.14) depends smoothly on η , one can run a ‘movie’ in η , diagonalizing the Hamiltonian in TCSA for different values of η from 0 to 1. As shown in Figure 5.1, the energy of the set of runaway

states first moves upwards, but then turns back and comes down to form the spectrum of the endpoint $\text{DSG}_2^{\eta=1} = \text{SG}(\beta/2, 1)$.

We wish to note that the runaway states do not eventually cross the other lines; rather, there are line avoidances which is a typical pattern for states that are metastable in finite volume and eventually decay [10] (see also [9] for similar results for the off-critical Ising model in magnetic field).

Let us now discuss what happens for general δ . Specializing (4.13, 4.21, 4.22), we obtain

$$\delta\mathcal{E}^{(0)} = -\delta\mathcal{E}^{(1)} = -\lambda\mathcal{G}_{\beta/2}(\beta)\cos\delta \quad (5.12)$$

$$\delta M_1^{(0)} = -\delta M_1^{(1)} = \frac{\lambda\mathcal{G}_{\beta/2}(\beta)}{M_\beta}\mathcal{N}\cos\delta\exp\left\{-\frac{1}{\pi}\int_0^{p\pi}dt\frac{t}{\sin t}\right\} \quad (5.13)$$

$$\delta M_2^{(0)} = -\delta M_2^{(1)} = \frac{\lambda\mathcal{G}_{\beta/2}(\beta)}{M_\beta}\mathcal{N}^2\cos\delta\frac{3\cos^2\left(\frac{p\pi}{2}\right)-1}{\cos p\pi}\exp\left\{-\frac{2}{\pi}\int_0^{p\pi}dt\frac{t}{\sin t}\right\} \quad (5.14)$$

Note that at $\delta = \frac{\pi}{2}$ the $O(\lambda)$ corrections vanish and in particular the two vacua become degenerate. We shall show shortly that this is also true nonperturbatively, at least as long as η is smaller than some critical value η_{crit} .

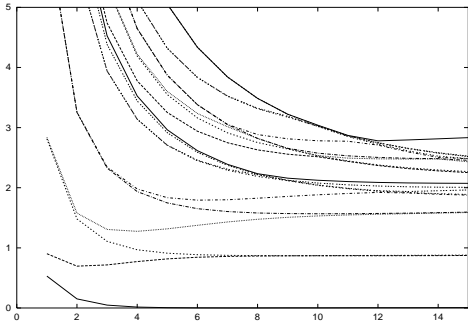
Now we proceed to the comparison between FFPT and TCSA, using plots. The first order corrections are linear in the coupling constant of the perturbing operator, so to use a convenient and dimensionless parametrization, we define the following combination:

$$\hat{\lambda} = \lambda M_\beta^{-x_\beta} . \quad (5.15)$$

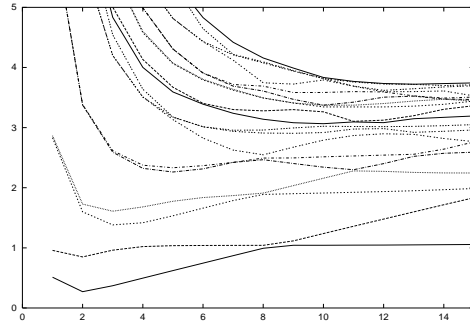
Figure 5.2 shows the results for the correction to the vacuum energy density $\delta\mathcal{E}_{\text{vac}}/M_\beta^2$ for $\delta = 0$ and $\beta = 4\sqrt{\pi}/3$, in units of the soliton mass M_β . The agreement is spectacular for a quite long range of the coupling. Similarly, Figure 5.3 shows the breather mass corrections for the four particles $B_1^{(0)}$, $B_2^{(0)}$, $B_1^{(1)}$ and $B_2^{(1)}$ at the same values of β and δ . For comparison we have also plotted the classical prediction for $\delta M_1^{(0)}$. Finally, Figure 5.4 presents the dependence of the mass corrections on the phase parameter δ at a suitably small value of $\hat{\lambda}$. (Note that here, to ensure better visibility, we changed the scale on the vertical axis with respect to Figure 5.3. As a result, the deviation between the first order FFPT and the TCSA results is much more pronounced).

One can also check the agreement between TCSA and FFPT for a perturbation theory in the coupling μ , i.e. around $\eta = 1$. The results are similar, except that the validity range of first order perturbation theory is smaller than around $\eta = 0$. The dependence of the first and second breather masses on η is shown in Figure 5.5.

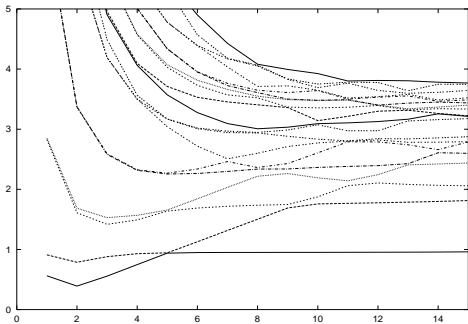
To sum up, the comparison between TCSA and FFPT gives a convincing evidence for the validity of both approaches in the perturbative ($\eta \sim 0$ or $\eta \sim 1$) domain. This is of utmost importance because for the purposes of further investigations we shall continue to use TCSA inside the complete interval $0 < \eta < 1$, where there are no ways to check its validity by any independent method (except some semiclassical analysis and qualitative arguments).



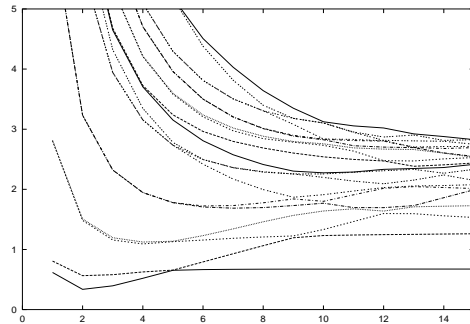
(a) $\eta = 0$



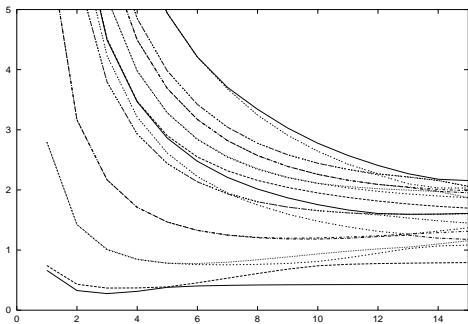
(b) $\eta = 0.2$



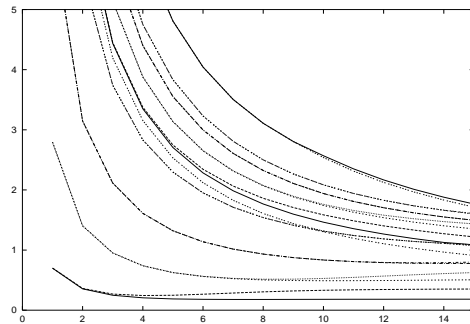
(c) $\eta = 0.4$



(d) $\eta = 0.6$



(e) $\eta = 0.8$



(f) $\eta = 1$

Figure 5.1: Change of the spectrum as η varies from 0 to 1 in DSG_2^η for $\beta = 4\sqrt{\pi}/3$ and $\delta = 0$. The energies are normalized by subtracting the ground state contribution. The plots show the first 20 states (including the ground state, which has constant zero energy in this convention).

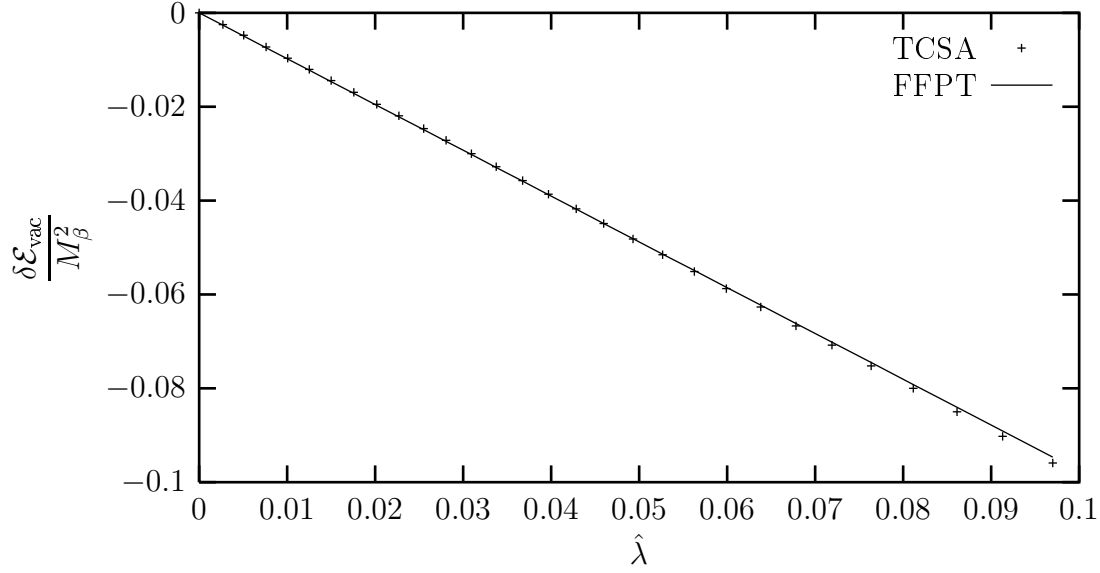


Figure 5.2: The correction to the vacuum energy density as a function of $\hat{\lambda}$

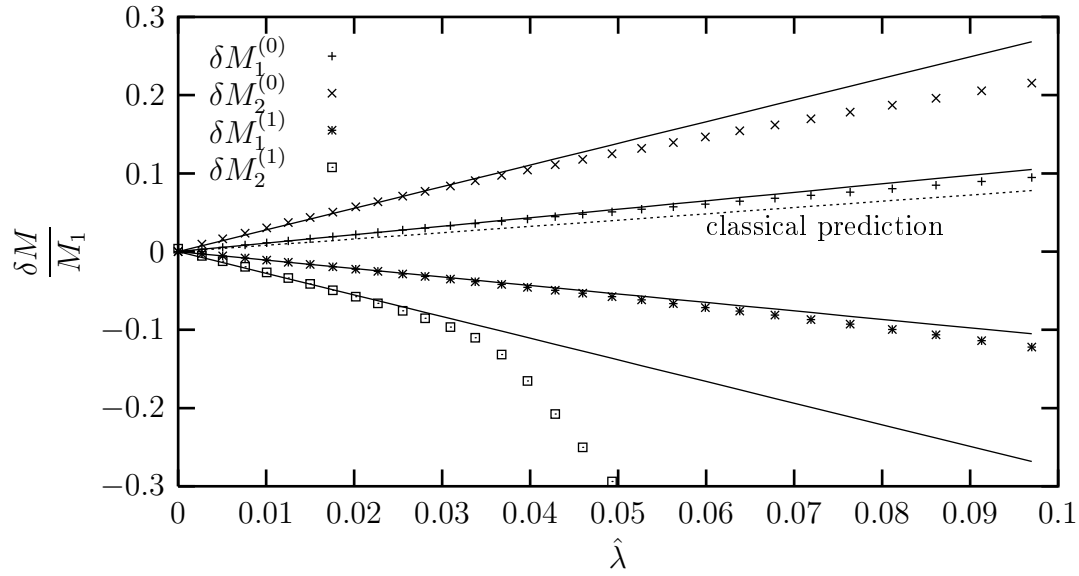


Figure 5.3: Breather mass corrections as functions of $\hat{\lambda}$

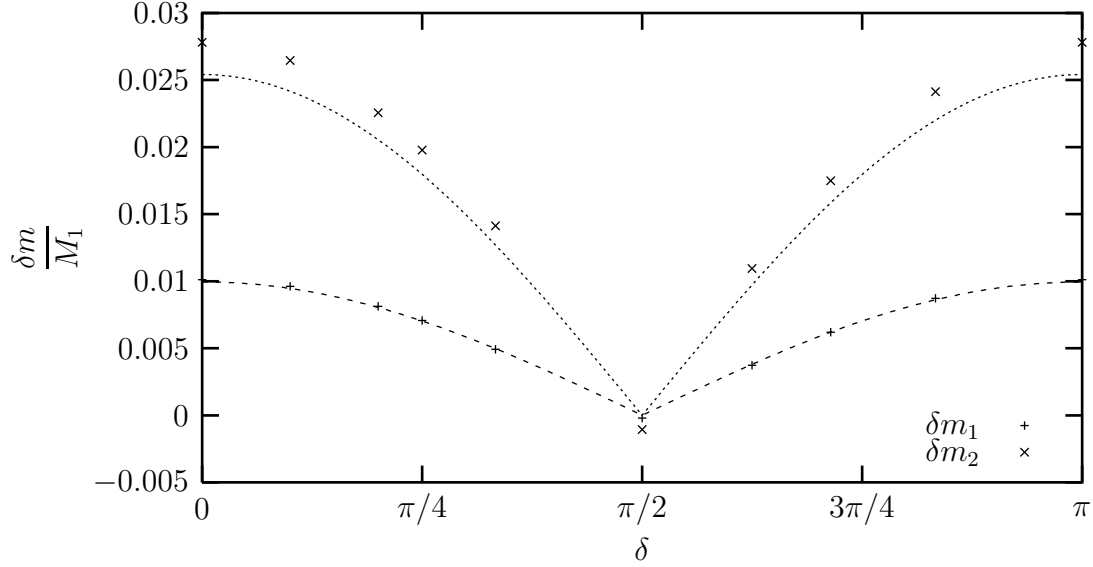


Figure 5.4: Breather mass corrections as functions of δ at $\hat{\lambda} \approx 0.01$ and $\beta = 4\sqrt{\pi}/3$

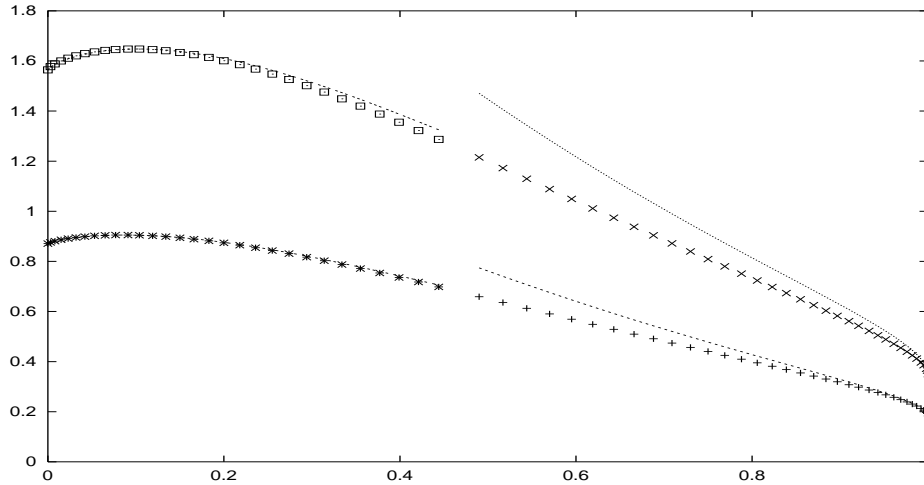


Figure 5.5: The dependence of the first and second breather masses on η running from 0 to 1 in $\text{DSG}_2^\eta(4\sqrt{\pi}/3, 0)$. The dots are the numerical TCSA data while the lines are the perturbative results obtained by using FFPT around the two endpoints $\eta = 0$ and $\eta = 1$.

6 Phase transition in DSG_2^η : generalities

We now turn to examining the phase diagram of the theory DSG_2^η as η varies from 0 to 1. We have seen that the theory has two degenerate vacua at $\eta = 0$, while there is only one ground state at $\eta = 1$. This hints at the possibility of a phase transition happening somewhere in between. However, for generic values of the parameters the degeneracy between the two vacua is lifted as soon as $\eta > 0$ thus the end point $\eta = 0$ is singular in this sense.

However, as we have already pointed out (subsection 5.2) the first order corrections to the vacuum energy densities (5.12) vanish exactly when δ takes a value on the boundary of its fundamental range

$$\delta = \frac{\pi}{2}. \quad (6.1)$$

From now on we restrict ourselves to this special value of δ and by a slight abuse of notation denote this model by DSG_2^η .

In this section we present an argument that the energy difference between the two vacua eventually vanishes to all orders in λ and that there is a critical value $\eta = \eta_{\text{crit}}$ at which there is a second order phase transition. Since all perturbative corrections to the vacuum energy difference vanish, this transition is entirely in a nonperturbative regime and form factor perturbation theory is not applicable. We first present a semiclassical (mean field/Landau-Ginzburg) analysis, extending the arguments given by Delfino and Mussardo [1] and Fabrizio et al. [2], and discuss the signatures of first and second order phase transitions in finite volume. In the next section we use TCSA to verify the predictions of the semiclassical considerations and in particular to establish the second order nature of the phase transition and its corresponding universality class.

6.1 Landau-Ginzburg analysis

We start our analysis with the classical potential

$$\begin{aligned} V(\Phi) &= -\mu \cos \beta\Phi - \lambda \cos(\alpha\Phi + \delta) \\ &= -\mu \cos \beta\Phi + \lambda \sin\left(\frac{\beta}{2}\Phi\right). \end{aligned} \quad (6.2)$$

For definiteness, let us suppose that μ and λ are positive without losing generality. As the potential is periodic under $\Phi \rightarrow \Phi + 4\pi/\beta$, the fundamental range of the field variable can be taken as

$$-\frac{3\pi}{\beta} \leq \Phi < \frac{\pi}{\beta}. \quad (6.3)$$

Note that the potential also has the discrete (\mathbb{Z}_2) symmetry

$$T : \Phi \rightarrow -\frac{2\pi}{\beta} - \Phi. \quad (6.4)$$

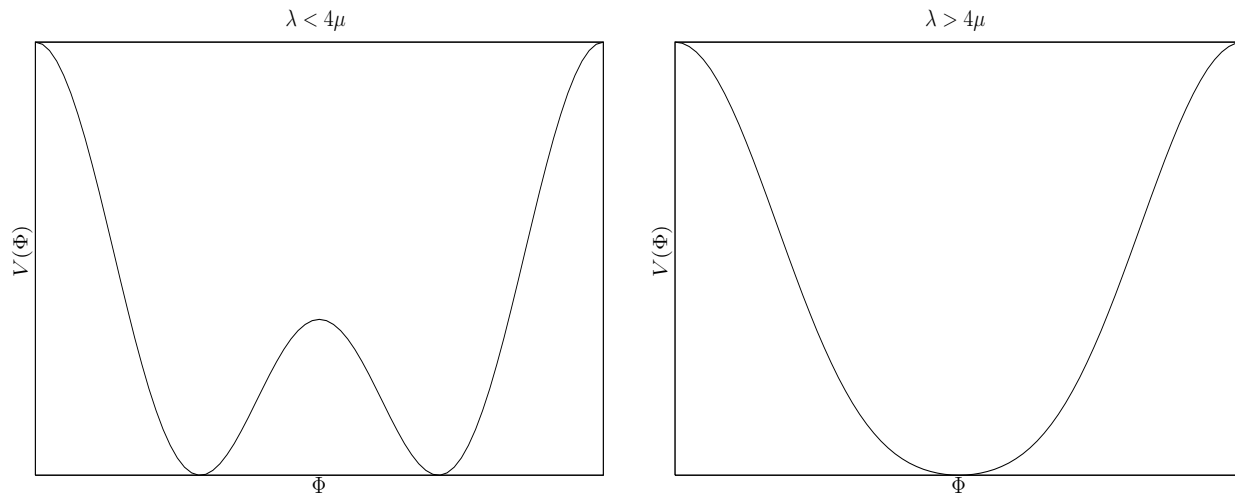


Figure 6.1: The behaviour of the classical potential $V(\Phi)$ for $\lambda < 4\mu$ and $\lambda > 4\mu$

Then a simple analysis establishes that the potential shows the characteristics of a second order phase transition at the point $\lambda = 4\mu$ (see Figure 6.1). Since classically the dimensions of μ and λ are $x_\alpha = x_\beta = 2$, the definition (3.11) of η reduces to

$$\eta = \frac{\lambda^2}{\mu^2 + \lambda^2} \quad (6.5)$$

and so this point corresponds to the following critical value of η

$$\eta_{\text{crit}}(\beta = 0) = \frac{16}{17} = 0.941\dots \quad (6.6)$$

In view of the \mathbb{Z}_2 symmetry (6.4) one would like to conclude that this is a second order phase transition point in the Ising universality class. However, there is a caveat here, as discussed by Fabrizio et al. [2].

The essence of the problem can be summarized as follows. The potential $V(\Phi)$ is renormalized at the quantum level. To determine the phase structure, one needs to look at the effective potential. Due to the periodicity and the \mathbb{Z}_2 symmetry, it can be readily checked that the only possible new terms are of the form

$$\cos(r\beta\Phi), \quad r \in \mathbb{Z} \quad \text{or} \quad \sin(r\beta\Phi), \quad r \in \mathbb{Z} + \frac{1}{2}. \quad (6.7)$$

The conformal dimensions of these operators are

$$\Delta_r^\pm = \frac{r^2\beta^2}{8\pi}, \quad (6.8)$$

and so as one increases r they are less and less relevant. The first two possibilities are particularly interesting. Fabrizio et al. [2] claim that while $\sin(\frac{3\beta}{2}\Phi)$ has no effect on the

nature of the phase transition (apart from modifying the position of the critical point), the term $\cos(2\beta\Phi)$ which is a relevant perturbing operator for $\beta^2 < 2\pi$ can (depending on its coefficient) turn the second order phase transition into a first order one.

Let us analyze the effect of such operators now. We take as our quantum effective potential the expression

$$V_{\text{eff}}(\Phi) = -\mu \cos \beta\Phi + \lambda \sin \frac{\beta}{2}\Phi + \kappa \sin \frac{3\beta}{2}\Phi + \nu \cos 2\beta\Phi . \quad (6.9)$$

κ and ν can eventually be expressed in terms of λ and μ , but their precise expressions are unknown. The conditions for the existence of a second-order phase transition point are

$$V_{\text{eff}}''(\Phi) \Big|_{\Phi=-\frac{\pi}{\beta}} = 0 \quad , \quad V_{\text{eff}}^{(4)}(\Phi) \Big|_{\Phi=-\frac{\pi}{\beta}} > 0 \quad , \quad (6.10)$$

since the \mathbb{Z}_2 symmetric extremum is at $\Phi = -\frac{\pi}{\beta}$.

Explicitly, we have the conditions

$$-4\mu + \lambda - 9\kappa - 16\nu = 0 \quad , \quad 16\mu - \lambda + 81\kappa + 256\nu > 0 . \quad (6.11)$$

Putting $\kappa = \nu = 0$ we recover that the phase transition point in the classical potential is at $\lambda = 4\mu$ and the second derivative is positive (we assumed that λ and μ are positive).

Suppose now that κ and ν are independent parameters and that we vary only λ . The critical point can be read off from the first condition in (6.11):

$$\lambda_c = 4\mu + 9\kappa + 16\nu . \quad (6.12)$$

Therefore the condition for a second order transition is

$$\mu + 6\kappa + 20\nu > 0 . \quad (6.13)$$

We can draw three conclusions. First, there is ample space for second order phase transition even in the presence of the higher frequency terms in the effective potential. Second, the term $\sin \frac{3\beta}{2}\Phi$ is also capable of inducing a first order transition, since a large negative κ is enough. Third, it is also possible that higher order derivatives vanish at the transition as well, giving tricritical and in fact even tetracritical points (even higher frequency terms open the possibility to multicritical points of any order). These observations can also be confirmed by simply plotting the effective potential for different values of the parameters.

However, for the double sine-Gordon model (2.1) the coefficients of the higher frequency terms (e.g. κ , ν) are fixed by the dynamics. Therefore this model lives on a specific surface in the multiparameter space of possible quantum effective potentials that respect the \mathbb{Z}_2 symmetry $\Phi \rightarrow -\frac{2\pi}{\beta} - \Phi$ and the periodicity $\Phi \rightarrow \Phi + 4\pi/\beta$. As we have already shown, the phase transition point is out of the reach of perturbative techniques and therefore one needs to recourse to some nonperturbative analysis to solve the problem. In the special case when $p = 1$ ($\beta^2 = 4\pi$), by using a mapping onto a generalized Ashkin Teller model, Fabrizio et al. [2] were able to show the existence of a second order phase transition. In

the general case, when $0 < p < 1$, since the model is nonintegrable, the only available candidate is TCSA (the upper limit is to avoid any UV problems with TCSA).

Finally we present the characteristic picture of a first order transition (see Figure 6.2). Since we disagree with the claim made by Fabrizio et al. that $\sin \frac{3\beta}{2}\Phi$ cannot induce a first order transition, we present a case in which it does. We fix the following values of the parameters

$$\kappa = -\frac{2}{5}\mu \quad , \quad \nu = 0, \quad (6.14)$$

and let λ vary from 0 upwards. At $\lambda = 0$, we have only the two vacua in which \mathbb{Z}_2 is spontaneously broken. At $\lambda = \frac{3}{5}\mu$ the symmetry preserving vacuum appears as a metastable state. For $\lambda = \frac{13}{8}\mu$ it becomes degenerate with the symmetry breaking vacua: this is the so-called coexistence point where the three vacuum states exist simultaneously in the theory. Then for $\lambda > \frac{13}{8}\mu$ the symmetric ground state becomes the true vacuum and the two other are metastable ones which disappear at $\lambda = \frac{61}{30}\mu$.

6.2 Signatures of 1st and 2nd order phase transitions in finite volume

In order to establish the nature of the phase transition we shall examine the spectrum of the model in a finite volume. To prepare the ground we now discuss the signatures of both types of phase transitions in the finite volume spectrum.

6.2.1 2nd order phase transitions

For definiteness we specify the symmetry of the transition to be \mathbb{Z}_2 , although the discussion can be easily generalized. In the broken phase, there are two degenerate vacua in infinite volume. For finite L the degeneracy is lifted by tunneling effects through the barrier separating them and the lowest lying becomes the ground state, while the other one is the first excited state. The split between the ground states vanishes exponentially as $L \rightarrow \infty$ because the height of the barrier is proportional to L . For $L \rightarrow 0$ the two ground states tend to some eigenstates of the conformal Hamiltonian and therefore the split is proportional to L^{-1} .

In the unbroken phase there is only one vacuum. The first excited state is generally some massive one-particle state and has a finite gap \mathcal{M} over the vacuum. Therefore the difference between the ground state and the first excited state tends to \mathcal{M} as $L \rightarrow \infty$ in the same way as indicated in eqn. (5.4).

Let us call the parameter in which the transition happens η_{crit} , in analogy with the DSG model. Then the characteristic behaviour can be summarized if we look at the mass gap \mathcal{M} as a function of η and suppose the unbroken phase is $\eta > \eta_{\text{crit}}$ while the broken one is $\eta < \eta_{\text{crit}}$. We have the following behaviour

$$\begin{aligned} \mathcal{M}(\eta) &= 0 \quad , \quad \eta < \eta_{\text{crit}} \\ \mathcal{M}(\eta) &> 0 \quad , \quad \eta > \eta_{\text{crit}} . \end{aligned} \quad (6.15)$$

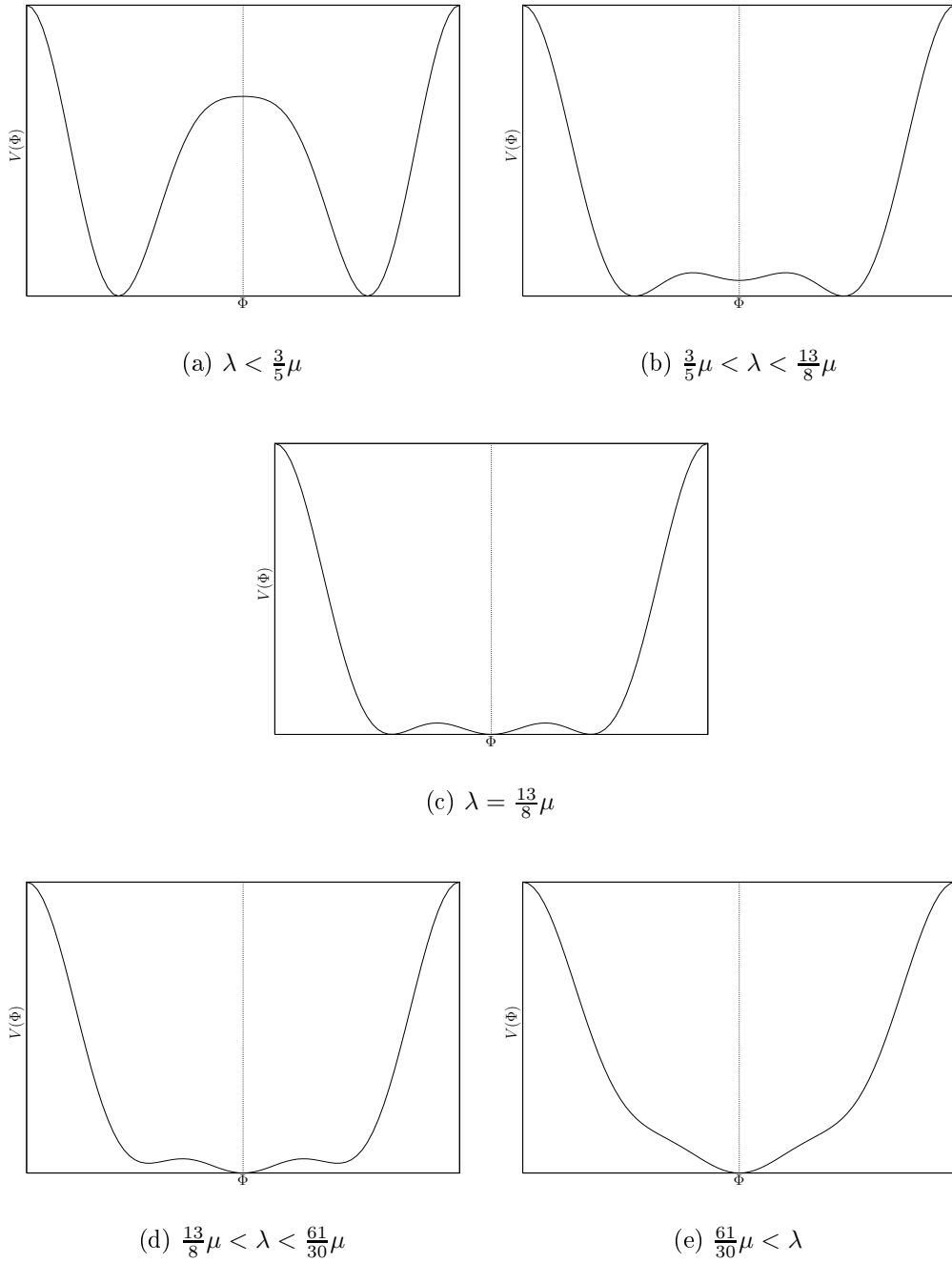


Figure 6.2: Illustrating a first order transition with $\kappa = -2/5\mu$ and $\nu = 0$

At exactly $\eta = \eta_{\text{crit}}$ by changing L from 0 to ∞ we interpolate between the UV $c = 1$ CFT and an IR fixed point one, which consists of an IR CFT and a massive one. Therefore certain states in the spectrum have the asymptotic (large L) behaviour

$$E_{\Psi}(L) - E_0(L) = \frac{2\pi (\Delta_{\text{IR}}^+ + \Delta_{\text{IR}}^-)}{L} + O(L^{-1-\epsilon}) \quad , \quad \epsilon > 0, \quad (6.16)$$

where the subscript 0 denotes the ground state (the lowest lying state in finite volume). These states fall into conformal families of the infrared fixed point characterizing the transition with conformal dimensions Δ_{IR}^{\pm} . As $L \rightarrow \infty$ they decouple from the rest of the spectrum which remains massive. The identification of such states allows the extraction of the characteristics of the infrared fixed point CFT as we shall see shortly.

6.2.2 1st order phase transition

A first order phase transition is always characterized by the existence of metastable states. As we have seen in Subsection 5.2, the existence of such states in finite volume implies that the space of states separates into excitations over the true ground state and those over the metastable ones which we called “runaway” states. The two sets of states have in general different bulk terms which coincide only when one tunes the coupling η to the coexistence point η_{coex} . At exactly this point the three vacua have identical energy densities and passing through this value of η the symmetry breaking pair of vacua interchanges with the symmetric one. This is a very characteristic behaviour which one would think is very easy to distinguish in the finite volume spectrum.

However, first order phase transitions have a characteristic strength and as is well-known, weak first order phase transitions are hard to distinguish from second order ones. To see this more concretely, let us denote the three vacua by Φ_0 for the symmetric one and Φ_{\pm} for the symmetry breaking ones, respectively. There are two other interesting points in η : the lower critical value η_{lcrit} where Φ_0 appears, and the higher critical value η_{hcrit} where Φ_{\pm} disappear as we increase η . In the case of a second order phase transition

$$\eta_{\text{lcrit}} = \eta_{\text{hcrit}}. \quad (6.17)$$

If the difference $\eta_{\text{hcrit}} - \eta_{\text{lcrit}}$ is small, then when tuning η numerically (or in an experiment) one may miss the existence of the metastable vacua. Similarly, one can look at the difference between the vacuum energy densities $V(\Phi_0) - V(\Phi_{\pm})$ at the lower and upper critical points. If it is small, then to detect the fact that the space of states separated into two sets of states with different linear terms in their energies one needs to go to very large values of the volume where truncation errors in TCSA become large. Therefore it is clear that one can never eventually distinguish a sufficiently weak first order transition from a second order one, neither numerically nor experimentally. An exact solution of the model would of course disentangle the problem, but given that the theory is not integrable this is too much to hope for.

7 The phase diagram in the case $\frac{\alpha}{\beta} = \frac{1}{2}$, $\delta = \frac{\pi}{2}$

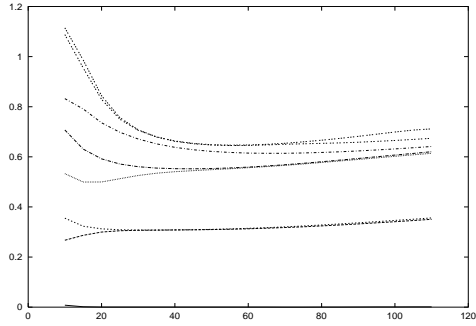
In this section we use TCSA to verify the classical predictions for the phase transition, and to clarify the order and the universality class of the transition. In order to check for the transition we need TCSA data over a wide range of the volume parameter l . Therefore, in order for TCSA to be useful, we have to restrict our investigations to the domain $\beta^2 < 4\pi$ where the method does not have UV divergences (see the discussion at the end of Subsection 3.2). It turned out that even in this range we cannot attain the necessary precision everywhere and to get a convergent enough numerical method we had to restrict $\beta^2 < 8\pi/3$. For the $\eta = 0$ sine-Gordon theory, this corresponds to a regime with two or more breathers in the spectrum.

To examine the nature of the phase transition we ran the η ‘movie’ with $\delta = \pi/2$ at various values of β . The results show no trace of a first order phase transition - a case is depicted on Figure 7.1. Indeed, for the case shown ($\beta = 8\sqrt{\pi}/7$) the spectra can be classified into three classes: (1) for $\eta < 0.8$ one can clearly see the doubly degenerate ground states and the also degenerate first massive states above them; (2) for $0.9 < \eta < 1$ the spectrum is massive, but there are no degeneracies among the lowest lying states and (3) in the transition domain, for $\eta \sim 0.84$, the structure of the spectrum changes, there are no lines tending to a constant, instead they decrease in the whole volume range and the degeneracies of the ground states and the first excited states are removed. Since at no place could we see the linearly rising set of runaway states that would correspond to the presence of metastable vacua with a different bulk energy, we analyze the data by looking for a 2nd order phase transition at some $\eta = \eta_{\text{crit}}$. (See however the remarks at the end of Subsection 6.2.2).

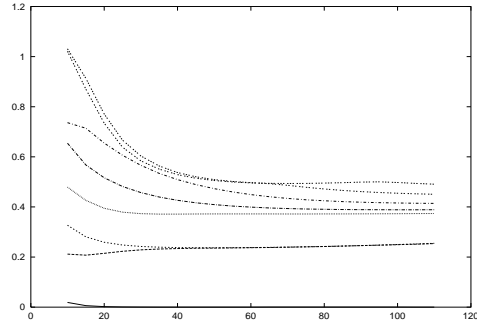
7.1 How do we find $\eta = \eta_{\text{crit}}$?

We determined the critical value of η in the following way: we tuned η in the transition region by looking for whether the $\epsilon_2(l) - \epsilon_{\text{vac}}(l)$ difference of the second excited state and the ground state continues to decrease along the (in between enlarged) complete l range. The meaning of this criterion is clear: this difference describes both at $\eta = 0$ and at $\eta = 1$ the mass of some low-lying breather of the limiting SG theories; thus its continuous decrease at a specific η_{crit} implies that this breather became massless. Since this happens only at this particular value of η , we think that this criterion is better than the one based on the appearance of a gap between the two ground states (as the gap is there for all $\eta > \eta_{\text{crit}}$). Nevertheless, for consistency, at η_{crit} chosen, $\epsilon_1(l) - \epsilon_{\text{vac}}(l)$ should decay slower than exponentially with l ; in fact, recalling eqn. (6.16), it should be $O(1/l)$ for large l .

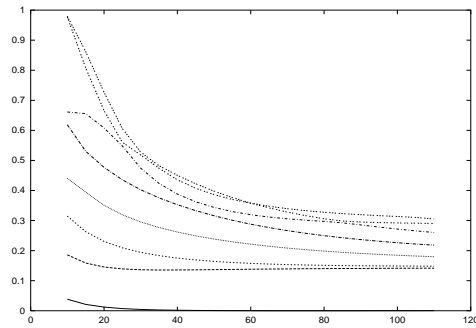
The result of this search is shown on Figures 7.2-7.4 for three different values of β . All three plots were taken at the ‘best’ η values according to our criterion. To separate more clearly the various $\epsilon_i(l) - \epsilon_0(l)$ as functions of l on all three plots we show these differences multiplied by $l/(2\pi)$. (This also makes them more suitable for the subsequent analysis). Here $\epsilon_0(l)$ denotes the lowest eigenvalue (vacuum energy) and i runs from 0 to



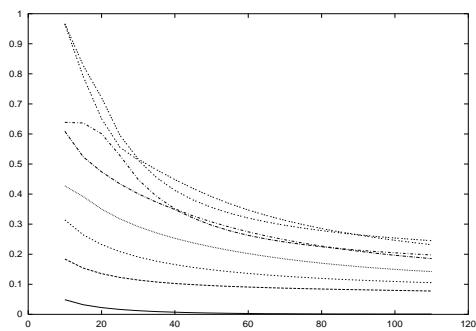
(a) $\eta = 0.6$



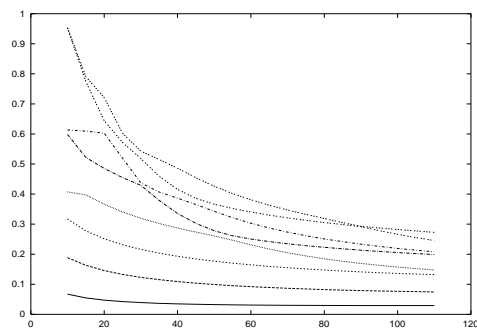
(b) $\eta = 0.7$



(c) $\eta = 0.8$



(d) $\eta = 0.84$



(e) $\eta = 0.9$

Figure 7.1: Change of the spectrum as η varies from 0 to 1 in DSG_2^η for $\beta = 8\sqrt{\pi}/7$ and $\delta = \pi/2$. The energies are normalized by subtracting the ground state contribution. The plots show the first 8 states.

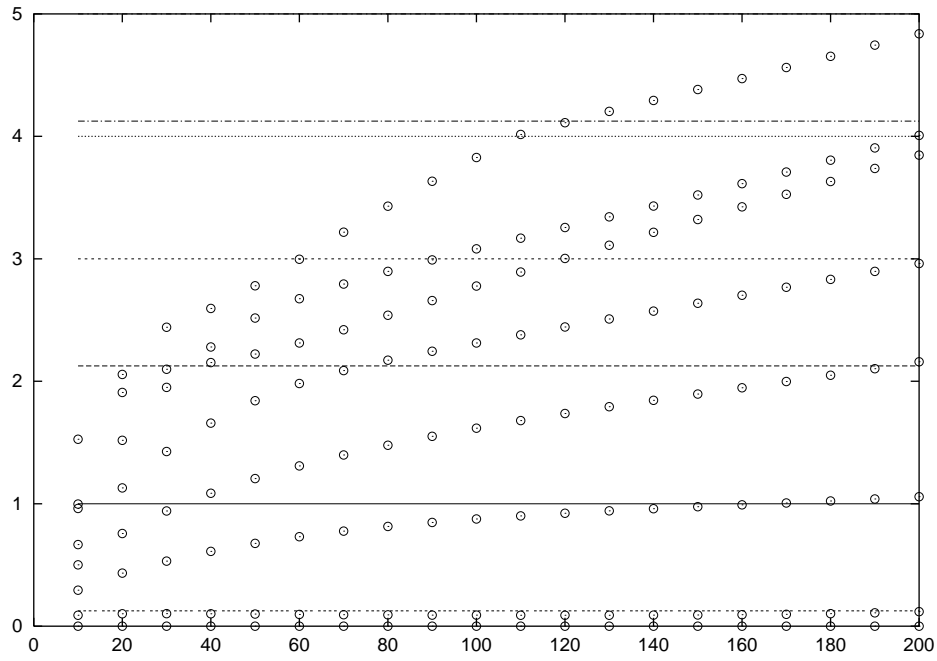


Figure 7.2: $[\epsilon_i(l) - \epsilon_0(l)]l/(2\pi)$ at $\beta = 8\sqrt{\pi}/7$ and $\eta = 0.866$

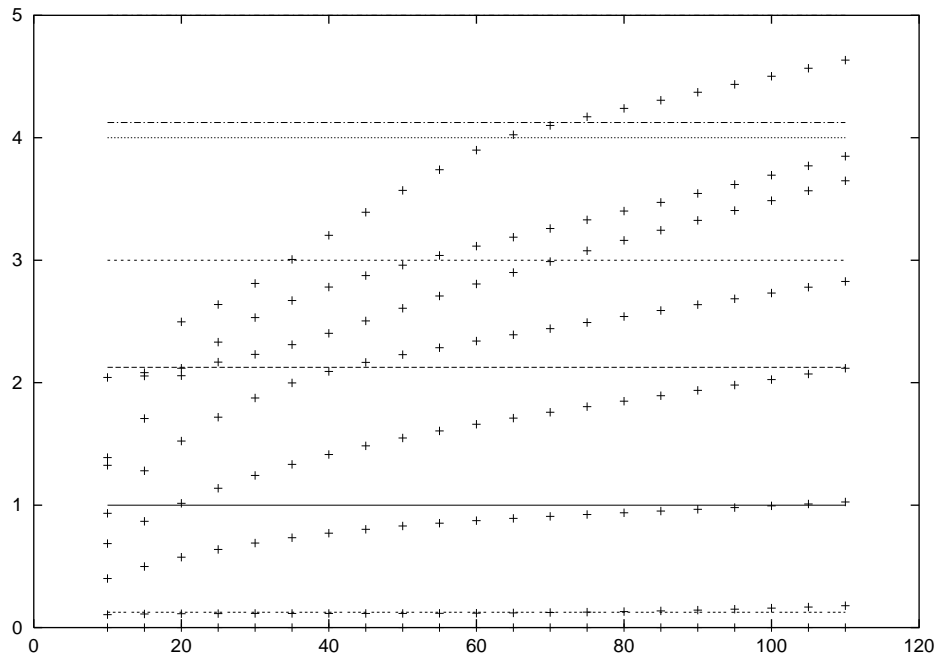


Figure 7.3: $[\epsilon_i(l) - \epsilon_0(l)]l/(2\pi)$ at $\beta = 4\sqrt{\pi}/3$ and $\eta = 0.850$

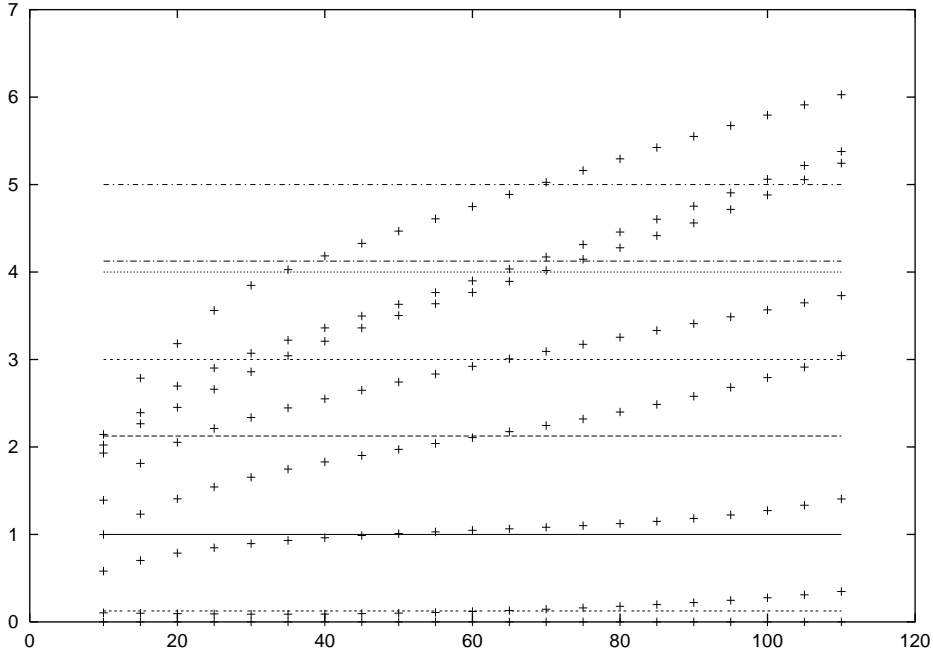


Figure 7.4: $[\epsilon_i(l) - \epsilon_0(l)] l / (2\pi)$ at $\beta = 8\sqrt{\pi}/5$ and $\eta = 0.838$

7. The horizontal lines on the plots correspond to the possible values of $\Delta_{\text{IR}}^+ + \Delta_{\text{IR}}^-$ if we assume that the IR CFT is the $c = 1/2$ Ising model (see eqn. (6.16)), when the spectrum of $\Delta_{\text{IR}}^+ + \Delta_{\text{IR}}^-$ is determined by the Ising primary fields and their descendants.

In all three cases we see that the first two lines - that correspond to the first two excited states above the ground state - qualitatively fit rather well to the Ising model's prediction. For the higher excited states the agreement is not so spectacular but even for them the sequence of lines and the absence of degeneracies (which on the Ising side follow from the null vector pattern) match that of the Ising prediction. For the two smaller β values it is clear that also some of the higher excited states would reach their corresponding plateaus by going to even higher volumes².

To make this agreement more quantitative we have to describe two types of effects. On the one hand we need the spectrum of states on the critical trajectory (i.e. at $\eta = \eta_{\text{crit}}$) in a finite volume more precisely than in eqn. (6.16), and on the other we need a clear, quantitative picture of the deviations from criticality since our best η may not equal η_{crit} (and TCSA errors may also be involved).

²These plots show that the higher the value of β the larger are the TCSA errors. The spectra were computed by using a conformal energy cut $E_{\text{cut}} \sim 15 - 16$ which resulted in $4.5 - 5.5 \times 10^3$ states in the UV conform Hilbert space.

7.2 Theoretical predictions for the form of the spectra

We describe these effects by assuming that the IR CFT is the critical Ising model, i.e. by using the Hilbert space and operator content of the Ising model.

Let us concentrate first on the finite volume corrections at $\eta = \eta_{\text{crit}}$. In this case when changing l from zero to infinity we interpolate from the UV conformal fixed point to an IR one, at least if we neglect the coupling between the massive and massless modes in the IR. The massive and massless modes decouple exactly at $l = \infty$ and we shall call the subspace of states asymptotically corresponding to the massless ones the *scaling sector*. Since one can flow into a fixed point only from an irrelevant direction, in this approximation the interpolating theory may be considered as an irrelevant perturbation of the conformal Ising model with (the non renormalizable) action

$$\mathcal{A} = \mathcal{A}_{\text{Ising}} + g \int d^2z (\psi(z, \bar{z}) + \text{higher dimensional fields}). \quad (7.1)$$

The various directions correspond to various choices of $\psi(z, \bar{z})$, which in turn are expressed in terms of the irrelevant (spinless and non vanishing) descendants of the primary fields. Since the DSG $_2^\eta(\beta, \pi/2)$ model exhibits the \mathbb{Z}_2 symmetry for all values of η , $\psi(z, \bar{z})$ may contain only the descendants of the energy operator $\partial\bar{\partial}\epsilon(z, \bar{z})$ +higher dimensional fields and of the identity operator $T\bar{T}$ +higher dimensional fields (where $\bar{T}(T)$ is the (anti)holomorphic component of the stress energy tensor of the Ising model). Recalling the generic form of the TCSA Hamiltonian,

$$H = \frac{2\pi}{L} \left(L_0 + \bar{L}_0 - \frac{c}{12} + \frac{gL^{2-2\Delta_\psi}}{(2\pi)^{1-2\Delta_\psi}} \hat{\psi}(1, 1) \right), \quad (7.2)$$

we see that for large but finite l the leading corrections to $E_\Psi(L) - E_0(L)$ come from the least irrelevant operator:

$$\epsilon_\Psi(l) - \epsilon_0(l) = \frac{2\pi}{l} (\Delta_{\text{IR}}^+ + \Delta_{\text{IR}}^-) + A_\Psi l^{1-2\Delta_\psi} + \dots \quad (7.3)$$

(Here the constant A may depend on the state in question). Thus, in our case, the leading correction takes the form

$$\epsilon_\Psi(l) - \epsilon_0(l) = \frac{2\pi}{l} (\Delta_{\text{IR}}^+ + \Delta_{\text{IR}}^-) + A_\Psi l^{-2} + \dots \quad (7.4)$$

if ψ is given by the derivative of the energy operator. (If this term were absent then $T\bar{T}$ would give a correction $\tilde{A}_\Psi l^{-3}$).

Numerically we can probably never tune η exactly to η_c , and even if we could the TCSA errors – coming from truncating the Hilbert space – would drive away from the critical trajectory connecting the UV and IR conformal theories. From the side of the Ising model this means that some relevant perturbation is also switched on, and we should also take its effects into account when discussing the large l spectrum. In the Ising model

there is only one relevant perturbation compatible with the \mathbb{Z}_2 symmetry, namely when the perturbing operator is $\epsilon(z, \bar{z})$. The presence of a relevant perturbation $\gamma\hat{\epsilon}(1, 1)$ in the TCSA Hamiltonian leads to a correction B_Ψ or $B_\Psi + C_\Psi l$ to $\epsilon_\Psi(l) - \epsilon_0(l)$ ³. Thus, summarizing, we expect, that in a large but finite volume range the energy spectrum can be described by the following:

$$\epsilon_i(l) - \epsilon_0(l) = B_i + \frac{2\pi}{l} D_i + A_i l^{-2} + C_i l + \dots \quad (7.5)$$

In the following we fit the TCSA data using this expression. We keep all these terms since we are at an intermediate volume range, where all of them can be equally important. A little bit more abstractly we can say that on the “best η ” trajectory we come into the vicinity of the IR fixed point, where the features of this CFT determine the energy spectrum, but eventually, because of the relevant perturbation, we are driven away and flow into a massive theory. Nevertheless, if in the intermediate volume range these expressions describe the spectra well, – in particular if the measured values of B_i (or B_i and C_i) are small and that of D_i are similar to the ones predicted by the Ising model – then this confirms the presence of a 2nd order phase transition in the Ising universality class. We call this intermediate volume range the *scaling region* which may (and in fact does, see Figures 7.2, 7.3 and 7.4) change from state to state.

Let us pause for a short discussion of the plateaus apparent in Figures 7.2, 7.3 and 7.4. Note that if we had the exact finite volume spectrum (i.e. without truncation errors) then the scaling functions

$$\frac{l}{2\pi} (\epsilon_i(l) - \epsilon_0(l)) \quad (7.6)$$

would tend to a constant as $l \rightarrow \infty$ for $\eta = \eta_{\text{crit}}$. In this sense the IR fixed point lies infinitely far away and the above functions approach asymptotic “plateaus” at $l = \infty$.

In the real TCSA situation, the scaling region corresponds to the plateaus in the numerical scaling functions. Tuning η closer and closer to the critical value these plateaus become longer and flatter and in addition they move to higher and higher values of the volume l .

Experience with TCSA for perturbed $c = 1$ CFTs shows that truncation errors generally decrease if one decreases β (or equivalently, increases the compactification radius of the conformal boson field). As a result of the above considerations, we expect that the plateaus are longer and flatter for smaller β and that they start at higher values of l . This is in fact what we observed in practice (see Figures 7.2, 7.3 and 7.4).

One can also make a theoretical prediction for the form of the energy $\epsilon_0(l)$ of the ground state as well. Using well-known facts about the off-critical Ising model [11] and arguments similar to the above one expects the following behaviour in the scaling region

$$\epsilon_0(l) = -\frac{\pi c}{6l} + a_0 l^{-2} + b_0 + c_0 l + \tilde{c}_0 l \log l + \dots \quad (7.7)$$

³The second term seems to be dominant over the first one, however its coefficient – which in a pCFT framework is of second order – in general is much smaller than the constant, thus for a large but finite range of l -s they may be equally important.

State	D_i	A_i	B_i	C_i
$i = 1$	0.125 ± 0.002	-1.2 ± 0.3	-0.0034 ± 0.0001	$1.45 \times 10^{-5} \pm 6 \times 10^{-7}$
$i = 2$	1.04 ± 0.03	-128 ± 8	0.0017 ± 0.0018	$9 \times 10^{-6} \pm 5 \times 10^{-6}$

(a) $\beta = 8\sqrt{\pi}/7$, $\eta = 0.866$

State	D_i	A_i	B_i	C_i
$i = 1$	0.1312 ± 0.0009	-1.35 ± 0.03	-0.0061 ± 0.0003	$2.6 \times 10^{-5} \pm 6 \times 10^{-6}$
$i = 2$	1.03 ± 0.02	-74 ± 3	0.005 ± 0.002	$1.4 \times 10^{-5} \pm 9 \times 10^{-6}$

(b) $\beta = 4\sqrt{\pi}/3$, $\eta = 0.850$

State	D_i	A_i	B_i	C_i
$i = 1$	0.1455 ± 0.0005	-0.89 ± 0.05	-0.0145 ± 0.0005	$2.24 \times 10^{-4} \pm 9 \times 10^{-6}$
$i = 2$	1.09 ± 0.02	-40 ± 2	-0.0015 ± 0.0031	$1.1 \times 10^{-4} \pm 2 \times 10^{-5}$

(c) $\beta = 8\sqrt{\pi}/5$, $\eta = 0.838$

Table 7.1: The results of fitting (7.5) to the first two excited states for various values of β at the estimated critical value of η

where $c = 1/2$ is the central charge of the Ising model and the logarithmic term appears as a result of a “resonance” between the linear (bulk) vacuum energy contribution and the perturbative corrections coming from the relevant operator ϵ . The term $\tilde{c}_0 l \log l$ is universal for all the excited states in the scaling sector and so disappears from energy differences like (7.5).

7.3 Numerical results

7.3.1 Scaling dimensions and UV-IR operator correspondence

One can fit the function (7.5) to the TCSA data in the scaling regions plotted in Figures 7.2, 7.3 and 7.4. The results of the fits are shown in table 7.1.

From the conformal data of the Ising fixed point we know that the first excited state should correspond to the spin operator σ with conformal dimensions $\Delta^\pm = 1/16$, while the second to the energy operator ϵ with conformal dimensions $\Delta^\pm = 1/2$. Therefore we expect

$$D_1 = \frac{1}{8} = 0.125 \quad , \quad D_2 = 1. \quad (7.8)$$

The data presented fit quite well with these predictions. Note that the agreement becomes better for smaller β where the TCSA errors are smaller. We mention that the errors

presented in the tables come from the fit procedure and do not contain the truncation errors which are generally much larger.

Another piece of information is the UV-IR operator correspondence. In TCSA we know the operator in the UV theory which creates the excited states. By identifying these states in the language of the IR theory, one can establish a correspondence between the UV and the IR operator content. In particular, the first and the second excited states are created by the operators

$$\cos \frac{\beta}{2}\Phi \quad \text{and} \quad \sin \frac{\beta}{2}\Phi \quad (7.9)$$

in the UV, respectively. In the IR these states flow to ones corresponding to the Ising operators σ and ϵ . This is in full accordance with their parity under the \mathbb{Z}_2 symmetry (6.4) and the fact that σ is an odd, while ϵ is an even operator in the Ising model. In addition, both the operator $\sin \frac{\beta}{2}\Phi$ in the DSG $^{\eta}$ model and the operator ϵ in the Ising case correspond to the “temperature” parameter deforming the model away from criticality. Furthermore, this conclusion also agrees with the conjecture made by Fabrizio et al. [2].

One could also try to extract the central charge c using the predicted form of the vacuum energy function (7.7). It turns out, however, that the fit is not sensitive enough to the value of c — in a least-squares algorithm the main contribution to χ^2 comes from the linear and $l \log l$ terms and c can only be determined with 30 – 40% accuracy, within which we find agreement with the Ising value $c = 1/2$.

7.3.2 Analysis of the phase diagram

Concerning the phase diagram, our first observation is that all evidence points to a second-order phase transition for all values of β , which happens at some critical value $\eta_{\text{crit}}(\beta)$ dependent on β . As we already discussed in Subsection 6.2, there is always a possibility of a sufficiently weak first order transition. The only statement one can make is that the phase transition is second order up to the precision within which the coefficients B_i and C_i in (7.5) vanish at the (approximate value of the) critical coupling. Given the data in table 7.1 and the fact that the normal precision in TCSA is of the order $10^{-2} - 10^{-3}$ for the values of the volumes used (this can be estimated e.g. calculating an integrable case when the exact values of the excited state energies are known) we can state that *the phase transition is second order up to the precision of the TCSA method.*

As we have already seen the second order nature of the phase transition is controlled by inequalities like (6.13). Since a very weakly first order transition requires a very weak breaking of these inequalities this in turn strongly constrains the parameters in the effective potential. However, the coefficients in the effective potential are uniquely determined in terms of λ and μ and therefore such a fine tuning is highly unlikely to happen.

It is expected that for $32\pi/9 < \beta^2 < 8\pi$ the transition is always second order since then all the possible corrections (6.7) to the effective potential correspond to irrelevant operators. Therefore it is only necessary to consider the case $0 < \beta^2 < 32\pi/9$. As TCSA is convergent for $\beta^2 < 4\pi$ it can be used to examine this range of couplings and all the

values of β were from this range. Unfortunately, TCSA does not converge very well for $\beta^2 > 8\pi/3$, so there is a gap in the values of β^2 up to $32\pi/9$ which is not accessible.

One also expects a second order transition around $\beta = 0$ since in this case the theory is semiclassical and the contributions to the effective potential are expected to be very small. We also know the exact value (6.6)

$$\eta_{\text{crit}}(\beta = 0) = \frac{16}{17} = 0.941\dots \quad (7.10)$$

Therefore we conjecture that *the phase transition in DSG_2^η is second-order for all values of β in the exact theory too.*

One can prepare a phase diagram in the (η, β) plane. For $\eta = 0$ the theory is in the broken symmetry phase, while for $\eta = 1$ the \mathbb{Z}_2 symmetry is restored. The phase transition line is described by a function $\eta = \eta_{\text{crit}}(\beta)$. One can also calculate the value of this function at the point $\beta = \sqrt{8\pi}$. For $\beta > \sqrt{8\pi}$ the term $\cos \beta\Phi$ becomes irrelevant and the theory is always in a symmetric phase. Therefore we expect that

$$\eta_{\text{crit}}(\beta = \sqrt{8\pi}) = 0. \quad (7.11)$$

Since the transformation $\beta \rightarrow -\beta$ can be compensated by a field redefinition $\Phi \rightarrow -\Phi$, one also has

$$\eta_{\text{crit}}(-\beta) = \eta_{\text{crit}}(\beta). \quad (7.12)$$

Figure 7.5 shows the phase diagram of the theory. The numerical data are the TCSA results for η_{crit} at particular values of β (in addition to the ones in Table 7.1, there is also a point with $\beta = 4\sqrt{\pi}/7$ where the measured critical coupling is $\eta_{\text{crit}} \approx 0.916 \pm 0.002$). The continuous line is an (even) polynomial interpolating the numerical data together with the two known values at $\beta = 0$ and $\sqrt{8\pi}$, which is shown in order to get an idea of the phase transition line. Below the transition line the theory is in the broken phase, while above the line the \mathbb{Z}_2 symmetry is restored.

8 Conclusions

In the present paper we examined the two-frequency sine-Gordon model, using a combination of various (analytic and numerical) approaches. Using form factor perturbation theory (FFPT) on the one hand and truncated conformal space approach (TCSA) on the other, we first verified the consistency of the two by comparing the results in the two perturbative regimes. Based on the agreement between the two methods, we continued to use TCSA in the nonperturbative regime.

Then we set up a framework for examining phase transition using the finite volume spectrum extracted from TCSA. We discussed how to distinguish between first and second order transitions, and in particular how to extract the characteristic quantities of an

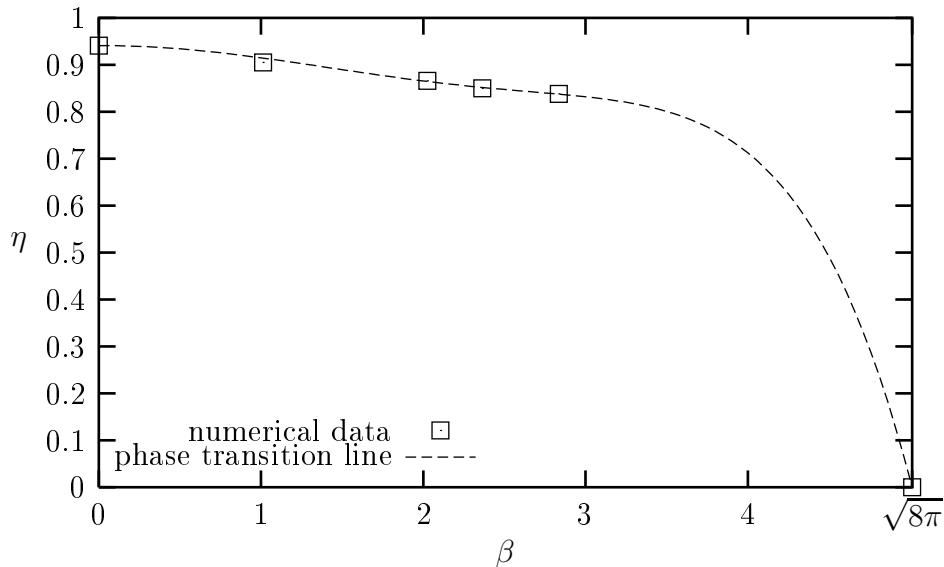


Figure 7.5: The phase diagram

eventual IR fixed point. To our knowledge this is the first case when TCSA was used for locating and characterizing a nontrivial fixed point. We would like to mention that TCSA was used before in the similar context of integrable massless flows in order to check results from Thermodynamics Bethe Ansatz (TBA) close to the UV CFT (small values of the volume l) [8]. Here, on the contrary, the TCSA method was used for finding the critical point at which the flow becomes massless and then analyzing the intermediate volume range in which the theory is governed by its IR fixed point. In addition, in our case there are no alternative nonperturbative methods since the theory is nonintegrable.

Using this framework, we examined the prediction by Delfino and Mussardo [1] of a second order phase transition, in a particular case when the ratio of the two frequencies was $1/2$. Contrary to a possibility raised by Fabrizio et al. [2] we argued that this phase transition is second order for *all* possible values of the sine-Gordon-like parameter β , at least within the precision attainable by TCSA. We examined the spectrum in detail and showed that the lowest lying states match the pattern of an Ising type fixed point, both qualitatively and quantitatively. We also examined the UV-IR operator correspondence and found an agreement with the conjectures made by Fabrizio et al.

In addition, by a simple mean field analysis we have shown that contrary to the claims made by Fabrizio et al., *all* lowest order correction terms to the effective potential are able to induce a first order transition, although the numerical studies suggest their coefficients are such that they do not affect the second-order nature of the transition in this particular case.

In this paper we restricted ourselves to the investigation of the vacuum sector. It could be interesting to see the effect of the phase transition in the topologically nontrivial sectors

as well. Another open question is to examine other possible frequency ratios and to extract the phase diagram for the general case. Yet another direction for further study is the case of irrational frequency ratios: as we already discussed in the paper, the perturbative approach (FFPT) is still applicable, but there are no nonperturbative alternatives at present. Finally, as the model has potentially interesting condensed matter applications, it is also a challenge to use the above framework to extract some quantities of interest in that context.

Acknowledgements

G. Takács would like to thank G. Mussardo for useful discussions. G. T. is supported by a PPARC (UK) postdoctoral fellowship, while Z. B. by an OTKA (Hungary) postdoctoral fellowship D25517. This research was also supported in part by the Hungarian Ministry of Education under FKFP 0178/1999 and the Hungarian National Science Fund (OTKA) T029802/99.

A Vacuum expectation values and breather form factors in (folded) sine-Gordon theory

Here we list the vacuum expectation values and form factors necessary for performing the form factor perturbation theory calculations in the main text, using the results in [12, 13]. We define our conventions for sine-Gordon theory with the action

$$\mathcal{A}_{SG} = \int dt \int dx \left(\frac{1}{2} \partial_\mu \Phi \partial^\mu \Phi + \mu : \cos \beta \Phi : \right). \quad (\text{A.1})$$

The vacuum expectation value of the exponential operator

$$V_a(x) = : \exp (ia\Phi(x)) : \quad (\text{A.2})$$

$$\mathcal{G}_a(\beta) = \langle 0 | V_a(0) | 0 \rangle \quad (\text{A.3})$$

is of the form [12]

$$\begin{aligned} \mathcal{G}_a(\beta) &= \left[\frac{M \sqrt{\pi} \Gamma \left(\frac{4\pi}{8\pi - \beta^2} \right)}{2\Gamma \left(\frac{\beta^2/2}{8\pi - \beta^2} \right)} \right] \\ &\times \exp \left\{ \int_0^\infty \frac{dt}{t} \left[\frac{\sinh^2 \left(\frac{a\beta}{4\pi} t \right)}{2 \sinh \left(\frac{\beta^2}{8\pi} t \right) \sinh(t) \cosh \left(\left(1 - \frac{\beta^2}{8\pi} \right) t \right)} - \frac{a^2}{4\pi} e^{-t} \right] \right\}, \quad (\text{A.4}) \end{aligned}$$

provided we normalize our operators in the following way:

$$\langle 0|V_a(x)V_{-a}(x')|0\rangle = \frac{1}{|x-x'|^{\frac{a^2}{4\pi}}} \quad \text{as } |x-x'| \rightarrow 0. \quad (\text{A.5})$$

Here M denotes the soliton mass and $|0\rangle$ is the vacuum in which the sine-Gordon field Φ has vanishing vacuum expectation value.

Let us use the following notations for the breather form factors

$$F_{k_1 \dots k_n}^{(a)}(\vartheta_1, \dots, \vartheta_n) = \langle 0|V_a(0)|B_{k_1}(\vartheta_1) \dots B_{k_n}(\vartheta_n)\rangle_0^{in}, \quad (\text{A.6})$$

where B_k denotes the k th breather with mass

$$M_k = 2M \sin\left(\frac{\pi k}{2}p\right) \quad , \quad p = \frac{\beta^2}{8\pi - \beta^2}. \quad (\text{A.7})$$

Then we have from [13]

$$F_{11}^{(a)}(\vartheta_1, \vartheta_2) = -\mathcal{G}_a(\beta)\bar{\lambda}^2[a]^2 R(\vartheta_1 - \vartheta_2), \quad (\text{A.8})$$

and

$$F_{1111}^{(a)}(\vartheta_1, \vartheta_2, \vartheta_3, \vartheta_4) = \mathcal{G}_a(\beta)\bar{\lambda}^4[a]^2 \prod_{1 \leq k < j \leq 4} R(\vartheta_k - \vartheta_j) \times \left\{ [a]^2 + (\sigma_1^2 \sigma_4 + \sigma_3^2) \prod_{1 \leq i < j \leq 4} (x_i + x_j)^{-1} \right\}, \quad (\text{A.9})$$

where we used the following notations

$$x_k = \exp(\vartheta_k) \quad , \quad [a] = \frac{\sin\left(p\pi\frac{a}{\beta}\right)}{\sin p\pi}, \quad (\text{A.10})$$

$$\bar{\lambda} = 2 \cos \frac{p\pi}{2} \sqrt{\sin \frac{p\pi}{2}} \exp\left(-\int_0^{p\pi} \frac{dt}{2\pi} \frac{t}{\sin t}\right), \quad (\text{A.11})$$

$$\sigma_1 = \sum_{i=1}^4 x_i \quad , \quad \sigma_4 = \prod_{i=1}^4 x_i \quad , \quad \sigma_3 = \sigma_4 \sum_{i=1}^4 x_i^{-1}, \quad (\text{A.12})$$

and in the strip $-2\pi + p\pi \leq \Im m \vartheta \leq -p\pi$ (note that in the attractive regime $p < 1$) the function $R(\vartheta)$ is defined as

$$R(\vartheta) = \mathcal{N} \exp \left\{ 8 \int \frac{dt}{t} \frac{\sinh(t) \sinh(pt) \sinh((1+p)t)}{\sinh^2 2t} \sinh^2 \left[\left(1 - \frac{i\vartheta}{\pi}\right) t \right] \right\}, \quad (\text{A.13})$$

with

$$\mathcal{N} = \exp \left\{ 4 \int \frac{dt \sinh(t) \sinh(pt) \sinh((1+p)t)}{t \sinh^2 2t} \right\} . \quad (\text{A.14})$$

$R(\vartheta)$ satisfies the useful identity

$$R(\vartheta) R(\vartheta \pm i\pi) = \frac{\sinh \vartheta}{\sinh \vartheta \mp \sin p\pi} \quad (\text{A.15})$$

which can be used to continue it analytically out of the validity range of its integral representation.

For the mass correction of the second breather we need the explicit form of the form factor $F_{22}^{(a)}$. This is not available in the literature, but can be computed from $F_{1111}^{(a)}$ using the bootstrap equation

$$i \operatorname{Res}_{\epsilon \rightarrow 0} F_{a_1 \dots a_n 11}(\vartheta_1, \dots, \vartheta_n, \vartheta_{n+1} + i\bar{U}_{12}^1 - \frac{\epsilon}{2}, \vartheta_{n+1} - i\bar{U}_{12}^1 + \frac{\epsilon}{2}) = \quad (\text{A.16})$$

$$\Gamma_{11}^2 F_{a_1 \dots a_n 2}(\vartheta_1, \dots, \vartheta_n, \vartheta_{n+1}) . \quad (\text{A.17})$$

The fusion angle \bar{U}_{12}^1 and the three-point coupling Γ_{11}^2 are defined from the B_2 pole U_{11}^2 in the $B_1 - B_1$ S -matrix:

$$S_{11}(\vartheta) \sim \frac{i(\Gamma_{11}^2)^2}{\vartheta - iU_{11}^2} , \quad \vartheta \sim iU_{11}^2 , \quad \text{where} \quad S_{11}(\vartheta) = \frac{\sinh \vartheta + i \sin p\pi}{\sinh \vartheta - i \sin p\pi} \quad (\text{A.18})$$

and from the relations

$$\bar{U}_{12}^1 = \pi - U_{12}^1 , \quad U_{11}^2 + 2U_{12}^1 = 2\pi . \quad (\text{A.19})$$

This way we find

$$U_{11}^2 = 2\bar{U}_{12}^1 = p\pi , \quad (\Gamma_{11}^2)^2 = 2 \tan p\pi . \quad (\text{A.20})$$

The residue of R can be calculated from (A.15)

$$R(-ip\pi + \epsilon) = -\frac{i}{\epsilon} \tan p\pi \frac{1}{R(-i\pi(1+p))} \quad (\text{A.21})$$

and finally the $B_2 - B_2$ form factor is

$$F_{22}^{(a)}(\vartheta_1, \vartheta_2) = (\Gamma_{11}^2)^{-2} K_{22}(\vartheta) R(\vartheta)^2 R(-\vartheta - ip\pi) R(-\vartheta + ip\pi) \frac{\tan^2(p\pi)}{R(-i\pi(1+p))^2} ,$$

$$K_{22}(\vartheta) = \mathcal{G}_a(\beta) \bar{\lambda}^4 [a]^2 \left\{ [a]^2 + \frac{1}{\cosh(\vartheta) + \cos(p\pi)} \right\} , \quad \vartheta = \vartheta_1 - \vartheta_2 . \quad (\text{A.22})$$

Finally we recall that in the perturbative investigation of the DSG model we need the vacuum expectation values and form factors in the sectors over the vacua $|k\rangle$ characterized by the property

$$\langle k | \Phi(x) | k \rangle = \frac{2\pi}{\beta} k. \quad (\text{A.23})$$

Using the following symmetries of the folded sine-Gordon model

$$\Phi \rightarrow \Phi + \frac{2\pi}{\beta}, \quad \Phi \rightarrow -\Phi, \quad (\text{A.24})$$

it can be easily shown [7] that

$$\mathcal{G}_a^{(k)}(\beta) = \langle k | V_a(0) | k \rangle = \mathcal{G}_a(\beta) e^{i\frac{2\pi a}{\beta} k}. \quad (\text{A.25})$$

The form factors corresponding to states above these vacua can be obtained by substituting $\mathcal{G}_a(\beta)$ with $\mathcal{G}_a^{(k)}(\beta)$ in the form factor formulae (A.8, A.9, A.22) above.

References

- [1] G. Delfino and G. Mussardo, *Nucl. Phys.* **B516** (1998) 675-703, hep-th/9709028.
- [2] M. Fabrizio, A. O. Gogolin and A. A. Nersesyan, *Nucl. Phys.* **B580** (2000) 647-687, cond-mat/0001227.
- [3] R.K. Bullough, P.J. Caudrey and H.M. Gibbs, in *Solitons*, Eds. R.K. Bullough and P.J. Caudrey, Topics in Current Physics v. 17, Springer-Verlag, 1980.
- [4] Al. B. Zamolodchikov, *Int. J. Mod. Phys.* **A10** (1995) 1125-1150.
- [5] V. P. Yurov and Al. B. Zamolodchikov, *Int. J. Mod. Phys.* **A6** (1991) 4557-4578.
- [6] G. Feverati, F. Ravanini and G. Takács, *Phys. Lett.* **B430** (1998) 264-273, hep-th/9803104.
G. Feverati, F. Ravanini and G. Takács, *Nucl. Phys.* **B540** (1999) 543-586, hep-th/9805117.
- [7] Z. Bajnok, L.Palla, G. Takács and F. Wágner: *The k-folded sine-Gordon model in finite volume*, ITP-BUDAPEST-557, KCL-MTH-00-21, hep-th/0004181, to appear in *Nucl. Phys.* **B**.
- [8] T.R. Klassen and E. Melzer, *Nucl. Phys.* **B370** (1992) 511-550.
- [9] G. Delfino, G. Mussardo and P. Simonetti, *Nucl. Phys.* **B473** (1996) 469-508, hep-th/9603011.

- [10] M. Lüscher in *Champs, cordes et phenomenes critiques*, Proc. Les Houches Summer School, ed. E. Brezin and J. Zinn-Justin (North-Holland, Amsterdam, 1989).
- [11] T.R. Klassen and E. Melzer, *Nucl. Phys.* **B350** (1991) 635-689.
- [12] S. Lukyanov and A.B. Zamolodchikov, *Nucl. Phys.* **B493** (1997) 571-587, hep-th/9611238.
- [13] S. Lukyanov, *Mod. Phys. Lett.* **A12** (1997) 2543-2550, hep-th/9703190.